JOURNAL *of the*

BOSTON SOCIETY OF CIVIL ENGINEERS

1848
BOSTON
SOCIETY
OF CIVIL
ENGINEERS

123 YEARS
1848 - 1971

VOLUME 58 JULY — 1971 NUMBER 3

JOURNAL OF THE
BOSTON SOCIETY
OF
CIVIL ENGINEERS

Volume 58 JULY 1971 Number 3

CONTENTS

Second-Class postage paid at Boston, Massachusetts

Published four times a year, January, April, July and October, by the Society
47 Winter Street, Boston, Massachusetts 02108

Subscription Price $10.00 a Year (4 Copies)
$2.50 a Copy
All orders must be accompanied by check

JOURNAL OF THE
BOSTON SOCIETY OF CIVIL ENGINEERS

Volume 58 JULY 1971 Number 3

A NEW LOOK AT SEDIMENTATION IN TURBULENT STREAMS

by

ARTHUR T. IPPEN,* Past President

(1971 John R. Freeman Memorial Lecture, presented before the Boston Society of Civil Engineers and the Hydraulics Section on February 17, 1971.)

Preliminary Remarks

The field of sedimentation in all its facets has been a most important one in scientific exploration through the years due to its significant role in many modern technologies and in all measures of human interference in natural flow processes. On the one hand we seek to lower the cost of bulk transportation by conveying materials such as coal, ore, grain, sand, gravel and silt in overland pipelines over short or very long distances. On the other hand we dislocate large sediment masses by agricultural practices, by deepening or realigning river channels and estuaries, by mining and exploiting sediment deposits, by denying natural deposition areas to our streams when floods are controlled by reservoirs, by dikes and land reclamation in flood plains. Many engineering plans often hastily conceived and executed did not anticipate nature's reaction in the form of erosion and deposition of large masses of sediment and consequently did not result in the hoped-for benefits.

To this day our understanding of the natural dynamic processes in sediment movement remains essentially one of empirical trial and error with regard to quantitative predictions, although the last fifty years have seen the development of many qualitative criteria through laboratory research and experimentation as well as through extensive field studies. Gross production of sediment from the watersheds of the United States alone exceeds 4 billion tons per year from all natural causes such as surface erosion, stream bank cutting, channel bed degradation and landslides. As yet in this overall figure, man's contribution through mining, industrial and domestic wastes, roads, housing and land clearing generally is relatively small, but nevertheless important and costly in his various development schemes. Individual projects in various countries have been seriously affected by the changes in sedimentation patterns produced by engineering measures with major side effects on the adjacent environment.

*Institute Professor and Director, Ralph M. Parsons Laboratory for Water Resources and Hydrodynamics, Department of Civil Engineering, Massachusetts Institute of Technology.

As an example from the most recent months the completion of the giant Aswan Dam in Egypt may be cited. For thousands of years the Nile delta people depended on the annual floods for their agricultural production. The deposition of the Nile's sediment in Lake Nasser will now disturb the equilibrium in the downstream portion of the river and cause a degradation in its bed by erosion, lowering gradually the water surface of the stream and in the adjacent underground. Similar experiences were reported on the Colorado River after the completion of Hoover Dam. Changes in the water quality are also incurred and Egyptian planners are now faced with new environmental challenges as the result of Aswan Dam.

While it is tempting to evaluate these consequences for the environment for which major changes in the sedimentation processes in river valleys are responsible, the task for this lecture must of necessity be more restricted. It will be more narrowly concerned with some of the mechanical features of sediment transport and, as much as feasible, dwell on some of the more recent research results in this difficult field. A word of warning is in order here, however. The literature on the various aspects of sedimentation is so vast and the purpose of the investigations digress so greatly depending on professional motivations that it is virtually impossible to relate a summary such as this to more than a specific theme. This restriction is also indicated by the complexity of the basic processes involved and it seems more worthwhile to deal with one of these more thoroughly than to resort to a superficial overview. In any case, excellent summaries have been published before and particular reference may be made in this connection to the various reports issued by the Committee on Sedimentation of the Hydraulics Division of the A.S.C.E. [1] and to the recent book by W. H. Graf [2].

Fundamentals of Bed Load Transport

Only the most important parameters for sediment transport as they have been established by analysis may be mentioned here. Amongst these the fall velocity w of a sediment grain of a given diameter in still water ranks prominently. It appears mostly in relation to the so-called shear velocity U_* which is defined through the bottom shear stress τ_0 by $U_*^2 = \tau_0/\rho = g\, y_0\, S_0$ in which ρ is the density, g is the acceleration of gravity, y_0 is the total depth, and S_0 the bottom gradient or energy gradient of a stream under steady uniform flow conditions.

Next, the layer of flow near the boundary which is governed by viscous forces primarily and is therefore mostly referred to as the laminar sublayer δ' has become an important concept in relation to the mean particle diameter d. The ratio d/δ' can then be stated also in the form:

$$\alpha \frac{d}{\delta'} = \frac{U_* d}{\nu} \tag{1}$$

which combines the stream characteristic U_*, the kinematic viscosity ν with the particle diameter d into a useful Reynolds parameter expressing physically the relative magnitude of d versus δ'. The factor α is often given the value of 11.6 but may have other values after proper definition. It is assumed then that as long as d is smaller than δ' the turbulence of the stream will not affect the flat bed of the stream composed of particles of diameter d. If d becomes much larger than δ' it will affect the value of the shearstress τ_0 itself and determine the hydraulically effective roughness of the boundary.

Whether or not movement of bed particles results for given flow conditions, is influenced by a second dimensionless ratio which relates the shearstress τ_0 to the buoyant specific weight of the particles $(\gamma_s - \gamma)$ and to the mean diameter d. With $\gamma_s/\gamma = S$ the specific gravity, and with the density of the ambient fluid as $\rho = \gamma/g$, this parameter may be expressed as:

$$\frac{\tau_0}{(\gamma_s - \gamma)d} = \frac{\tau_0/\rho}{g(S-1)d} = \frac{U_*^2}{(g(S-1)d}$$

Shields [3] first combined the two ratios just defined into a general functional relation:

$$\frac{U_*^2}{gd\,(S-1)} = \phi\left(\frac{U_*^d}{\nu}\right) \tag{2}$$

He showed by extensive experimental evidence that unique values of the parameters in equation (2) determined the initiation of motion for the sediment grains on the bed. His entrainment function ϕ given graphically in the literature has become generally accepted in research and practice although somewhat different results have been obtained in more recent studies.

In summary then three parameters have been found to have general significance for sedimentation studies:

$$\left(\frac{U_*}{w}\right), \quad \left(\frac{U_*}{gd\,(S-1)}\right), \quad \left(\frac{U_*d}{\nu}\right)$$

A theory for sediment transport of universal application has so far however been impossible to formulate. In explanation of this state of affairs a short descriptive resume may be given as follows:

After the grains along a flat bed start moving in considerable quantity, the type of transport is referred to as bed-load movement. As the volume concentration in the layers adjacent to the bed increases, the motion consists of sliding, rolling, agitated intermingling and saltation. The flow exerts drag and lift forces on the particles, unknown interaction of the particles in high concentration takes place, and the highly turbulent zone adjacent ot the boundary exerts random impulses on the fluid-sediment mixtures. Statistical approaches seemed indicated and have been attempted, prominently so by H. A. Einstein [2]. But in essence the parameters discussed above were again the building blocks of the various functions derived for the rate of bed-load transport usually given as q_s in cu. ft./sec. ft. Experimental data and field data have seldom shown general correlation, even though certain equations and certain sets of data proved consistent for the particular flow conditions and sediment properties employed. Most sediment transport formulae for bed-load have therefore the general formulation:

$$S \cdot q_s = \frac{U_*^2}{g} \; f \left(\frac{U_* d}{\nu} , \frac{U_*}{w} , \frac{U_*^2}{gd\,(S-1)} \right) \tag{3}$$

The application of more specific empirical relationships to practical design is still at best an educated guess and requires considerable experience with specific field conditions. This is not to say that at various times there have not been very satisfactory solutions.

Other factors entering into a more detailed analysis are the complications introduced by mixtures of sediments which are sorted by their variable response to the dynamics of the flow near the boundary, so that all kinds of movement coexist, such as intermittent rolling, sliding, saltation and suspension. In turn the interaction of the moving sediment with the fluid flow modifies the state of turbulence, the boundary shear and the state of the mean flow itself.

The surface shape of the bed itself deforms in alluvial streams. For small values of the Froude Number $F = U/\sqrt{gy_o}$ an initially flat bed will fairly rapidly change to a rippled surface and at a later stage dunes will appear. As the flow rate and thus the Froude number is increased further towards a critical value $F = 1$ the dunes will be washed away and a flat bed reappears. When the flow is near critical however, standing waves are formed on the surface and so-called sandwaves appear at the bottom. These seem to grow with the surface waves until the latter break with considerable turbulence generation similar to the hydraulic jump, and the sandwaves are washed away also. These relatively slow processes are then repeated at another favorable location. In contrast to ripples measured in inches, sandwaves may reach a height of many feet. In supercritical flow, finally large dunes of long length in terms of depth are formed which move slowly in the upstream direction. It is clear that the rate of sediment transport varies greatly under all of these bed roughness conditions as the shearstress becomes non-uniform both in the direction of flow and laterally.

These phenomena are mentioned here in passing only to call attention to the difficulty of formulating a general theory of sediment transport. As beds may deform at different stages of river flow, thus modifying materially the stage-discharge relationships, the same discharge may occur for considerable periods of time over beds of different roughness. As floods pass, bed forms do not revert immediately to equilibrium conditions if equilibrium conditions do indeed exist except in the laboratory. Nevertheless reasonable progress has been achieved in recent years also in this difficult area on various specific streams by field research. In the theoretical analysis of certain characteristics of dune and anti-dune behaviour, the basic work of J. F. Kennedy [4] may be mentioned which has stimulated others to get involved. In view of the complexities cited, the field of bed-load movement has many challenges confronting it in future research.

The Transport of Suspended Sediment

Historical Remarks

In contrast to bed-load movement which is subject to all the poorly understood processes of the fluid-sediment interaction close to bottom boundary, the analysis of solid suspensions over the depth of the stream has been more successful. This area of study had been of interest to me at the beginning of my professional career over 37 years ago, and then again I became involved in it in more recent years through research conducted in our laboratory at M.I.T. Early in 1934 as a graduate student at the California Institute of Technology I was looking for a topic for a doctoral dissertation and Professor Von Karman suggested that I read a paper by Murrough P. O'Brien in the Transactions of the American Geophysical Union [5]. This paper had appeared the year before and contained the postulation of the equilibrium for the upward dispersion of sedimentary particles in a turbulent stream and their downward settling by gravity in differential form. What was needed as a next step was the introduction of a suitable velocity distribution law to define the distribution over the depth of the turbulent eddy viscosity or momentum transfer coefficient ϵ_m. This would permit the integration of O'Brien's relation which had been derived for suspended particles in liquids. Some years earlier Wilhelm Schmidt had established the corresponding condition for dust particles in the atmosphere [6].

Both authors assumed that at any depth of the stream y, the net downward settling rate of particles w of a given diameter d through a unit horizontal area, was equal to the net upward dispersion by turbulent mass exchange from the higher concentration levels below to the lower concentrations above. Thus they obtained the well know relation:

$$c \cdot w = -\epsilon_s \frac{dc}{dy} \tag{4}$$

in which c = volume concentration
w = settling velocity in ft./sec.
y = depth measured from the bottom boundary
and ϵ_s = kinematic mass exchange coefficient.

The subscript s for this coefficient is to indicate that a difference is assumed between ϵ_s and the momentum transfer coefficient ϵ_m usually termed the eddy viscosity. Both are normally connected by

$$\epsilon_s = \beta \, \epsilon_m . \tag{5}$$

For the sake of simplicity the factor β is usually assumed to be unity, an assumption justified for small particles by careful analysis of experimental evidence [1b] (pp. 62 and 72). At any rate other necessary assumptions in further developments make the use of $\beta = 1$ quite acceptable.

The simplest integration of equation (4) is accomplished by assuming ϵ_s as constant with respect to the depth y. To produce such uniform turbulence a simple experimental system can be designed consisting of a vertical cylinder with a stirring device agitating the liquid in the column. H. E. Hurst [7] in 1929 performed such experiments first using rotating vanes and fixed baffles. He found the sediment distribution to conform to the one predicted by the equation:

$$\ell n \frac{c}{c_a} = \frac{aw}{\epsilon_s} \left(1 - \frac{y}{a}\right) \tag{6}$$

in which a indicates a reference depth at which c_a is measured.

A much more extensive study was conducted by H. Rouse [8] a few years later in 1936 with screens oscillating vertically with different frequencies and amplitudes. His definition of the sediment characteristics as well as the extensive scope of his test program revealed many details of the sediment-fluid interactions and encouraged their study in laboratory flumes.

The Sediment Distribution in Turbulent Streams

If the concept of equation (4) is applied to the study of uniform flow in a wide rectangular channel, the following relations must be referred to:

$$\tau = \rho \, \epsilon_m \frac{du}{dy} \tag{7a}$$

which defines the local shear τ at any depth y in relation to the kinematic eddy viscosity ϵ_m, the density ρ and the velocity gradient. In steady uniform flow in wide channels, the shear stress τ is varying linearly from zero at the surface to the maximum τ_o at the bottom. Hence, neglecting the presence of sediment.

$$\tau = \tau_o \ (1 - \frac{y}{y_o}). \tag{7b}$$

Introduction of equations (7a) and (7b) into equation (4) gives the basic expression

$$\frac{dc}{c} = - \frac{w}{\epsilon_s} \ dy = - \frac{w \cdot du/dy}{\sqrt{\tau_o/\rho} \cdot \beta \sqrt{\tau_o/\rho} \, (1 - \frac{y}{y_o})} \tag{8}$$

With an appropriate function for the velocity distribution, this equation can be readily integrated. This was first done by the writer in 1934 in unpublished notes using the logarithmic velocity distribution law proposed by H. Krey in 1927 [9]. This relation was given by Krey in the form:

$$\frac{u}{U_{max}} = \frac{\ell n \, (1 + \frac{y}{a})}{\ell n \, (1 + \frac{y_o}{a})} \tag{9}$$

The length a is introduced as a small distance from the bottom and is defined from the expression given by Krey by the equation:

$$\frac{U_{max}}{U_*} = \frac{a \, U_*}{\nu} \ \ell n \ (1 + \frac{y_o}{a}) \tag{10}$$

Therefore equation (9) can be expressed also in the form

$$\frac{u - U_{max}}{U_*} = \left(\frac{aU_*}{\nu}\right) \ell n \ \frac{(1 + \frac{y}{a})}{(1 + \frac{y_o}{a})} \tag{11}$$

This relation was not developed by the writer until early in 1969 in this form [10]. It shows however that it is equivalent to the so-called Karman-Prandtl velocity defect relation established in 1934 after Krey's equations (9) and (10), which is:

$$\frac{u - U_{max}}{U_*} = \frac{1}{k} \ \ell n \ (\frac{y}{y_o}) \tag{12}$$

Neglecting the small distance a in equation (11) versus y and y_o under the logarithm, as was done in equation (12) before, a comparison of equations (11) and (12) then results in the equality:

$$\frac{1}{k} = \left(\frac{aU_*}{\nu}\right) \tag{13}$$

Calculating Values of $a \cdot U_*/\nu$ from experimental evidence in accordance with equation (10) gives indeed values very close to the average value of the Von Karman universal constant k stated usually as .40 for equation (12).

The velocity gradients are as follows from both equations (11) and (12)

$$\frac{du}{dy} = \left(\frac{aU_*}{\nu}\right) \frac{U_*}{(y + a)} \tag{14}$$

$$\frac{du}{dy} = \frac{1}{k} \frac{U_*}{y} \tag{15}$$

It may be added that the small distance a is proportional to the laminar sublayer thickness δ' which is defined often by $(\delta' U_*/\nu) = 11.6$, although smaller values of the constant are often quoted down to values of 4. Assuming $k = .40$, it is seen that equation (13) results in $(a \cdot U_*/\nu) = 2.5$. At any rate the distance a is of the order 10^{-3} to 10^{-4} for usual conditions of clear water flow.

Introducing equation (14) to express the velocity gradient, equation (8) may be integrated between the limits $y = y_o$ and $y = a$

$$\frac{c}{c_a} = \left[\frac{y_o - y}{y + a} \cdot \frac{2a}{y_o}\right]^{Z_1} = \left[\frac{y_o - y}{y_o - a} \cdot \frac{2a}{y + a}\right]^{Z_1} \tag{16}$$

wherein:

$$Z_1 = \frac{1}{\beta} \frac{w}{U_*} \left(\frac{aU_*}{\nu}\right). \tag{17}$$

This relation was first given by the writer in 1934/35 but has been modified slightly for ready comparison with the following equations.

With equation (15) the relation (8) results in the integrated form

$$\frac{c}{c_b} = \left[\frac{y_o - y}{y_o - b} \cdot \frac{b}{y}\right]^{Z_2} \tag{18}$$

in which a depth b has been assumed for reference and may be any depth for which the concentration has been measured. Equation (18) was first established by H. Rouse [11] in the years 1936/37 with the value of the exponent given by

$$Z_2 = \frac{1}{\beta} \frac{w}{U_*} \cdot \frac{1}{k} \cdot \qquad (19)$$

It may be noted that equations (17) and (19) are identical if the equality of $1/k = aU_*/\nu$ is assumed. If a reference concentration c_b for depth $y = b$ is determined from equation (16), and the ratio c/c_b is formed, the result agrees with equation (18). Near the bottom, good agreement of the concentration distributions with the equations is doubtful in any case. Krey's equation (9) for the velocity distribution gives zero velocity at the boundary while Von Karman specifically excluded the validity of the logarithmic velocity distribution near the boundary.

Relation Between the Coefficient k and Sediment Concentration

Experience since the publication of equation (18) has demonstrated that the concentration of particles near the wall has an important effect on the distribution of velocity as well as of sediment, a finding which is generally evaluated by determining the coefficient k. Large variations in k for velocity distributions in streams carrying relatively small concentrations of sediment have generally been established [12] [13]. Such large variations in k in the writer's opinion are due to the large concentrations of particles at the boundary which result in large variations of the effective viscosity μ' from the values μ for the clear ambient fluid.

H. A. Einstein [14] gave many years ago a well-known approximation for the variation of the dynamic viscosity μ' in terms of the clear fluid viscosity μ with particle suspensions of concentration C_o

$$\mu' = \mu \; (1 + 2.5 \; C_o) \qquad (20)$$

Eilers [15] established from experimental data a better correlation which was verified in one of our own studies [16].

$$\left(\frac{\mu'}{\mu}\right)^{1/2} = 1 + 2.5 \; C_o \; \frac{1}{2(1-1.35 \; C_o)} \qquad (21)$$

For the present purposes equation (20) may suffice to redefine the shear stress at the bottom boundary in terms of the maximum concentration C_o:

$$\tau'_o = \mu' \frac{du}{dy} = \mu \frac{du}{dy} (1 + 2.5\, C_o) \tag{22}$$

The sediment load in the stream also produces an increase in the shearstress over the clear water shear so that

$$\tau'_o = \gamma\, y_o\, S_o \left[1 + (S-1) \int_0^{y_o} \frac{c\, dy}{y_o}\right] \tag{23}$$

Since the integral simply expresses the mean concentration over the depth, this equation can be rewritten as

$$\tau'_o = \gamma\, y_o\, S_o \left[1 + C_m\, (S - 1)\right] \tag{24}$$

wherein $S = \gamma_s/\gamma_f$, the specific gravity of the sediment.

Combining equations (22) and (24) yields:

$$\frac{du}{dy} = \gamma\, y_o\, S_o \frac{1}{\mu} \left[\frac{1 + C_m\, (S - 1)}{1 + 2.5\, C_o}\right] \tag{25}$$

With $\gamma\, y_o\, S_o = \tau_o = \rho U_*^2$ for clear water this relation may be rewritten as

$$\frac{du}{dy} = \frac{U_*^2}{\nu} \left[\frac{1 + C_m\, (S - 1)}{1 + 2.5\, C_o}\right] \tag{26}$$

This equation represents the modification in the velocity gradient near the boundary with suspended sediment. For clear water, equation (14) may be used near the boundary with y of the order a:

$$\frac{du}{dy} = \frac{aU_*}{\upsilon} \cdot \frac{U_*}{y + a} = \frac{1}{k} \frac{U_*}{y + a} \tag{14}$$

From equations (26) and (14) that distance $(y + a) = a'$ for which the velocity gradients become equal is now defined. Further defining $1/k' = a' U_*/\nu$ it is seen that

$$\frac{a' U_*}{\nu} \quad \frac{1}{k'} \quad \frac{1}{k} \cdot \left[\frac{1 + 2.5\, C_o}{1 + C_m (S - 1)}\right] \tag{27}$$

Since the factor by which $1/k$ is multiplied is always larger than unity for the usual sediments, it follows that k' is always smaller than k or that a' is always larger than a. This statement is amply supported by experimental and field studies.

Through the Krey equation, the universal constant k of Von Karman is shown to be governed by the sediment concentrations near the boundary and is changed to smaller values of k' when multiphase flow exists. Similarity assumptions for the region of flow at considerable distance from the bottom remain quite acceptable for the usual small concentrations C_m when the inertial interactions of particles with the turbulent flow can be neglected.

Equation (27) permits a number of important observations with regard to suspended sediment transport.

1. The maximum concentrations C_o moving near the bottom affect primarily the value of k.
2. The mean concentrations C_m are usually much less than the maximum concentrations C_o and therefore should show little correlation with changes in k.
3. Large changes in k observed with suspensions of near neutrally buoyant particles are seen to depend on C_o, while the term C_m (S - 1) tends towards zero. Values of C_o are approximately equal to C_m.
4. The value of k is affected only by the maximum volume concentration of particles near the boundary, not by other properties of the particles such as diameter and size distribution. The effective viscosity depends only on concentration in first approximation. However, particle sizes are assumed to be of the order of a or δ' in diameter.
5. By plotting velocity distributions in the upper portion of the depth, the constant k' may be determined for streams carrying suspended load, and hence the absolute concentration C_o may be obtained.

The developments up to this point may be illustrated by a series of graphs. Figure 1 shows for comparison two velocity distributions plotted to linear scale, one for clear water and the other for a suspension of neutrally buoyant particles of C_o = .27. The characteristic decrease of the gradient near the boundary as well as its increase in the upper part of the depth is quite evident and stands confirmed by many experiments. When plotted to a semi-logarithmic scale the same runs show a straight line for the clear water with a value of k = .376, while for C_o = .27 the k' = .248 and a curve results over almost the entire depth (see

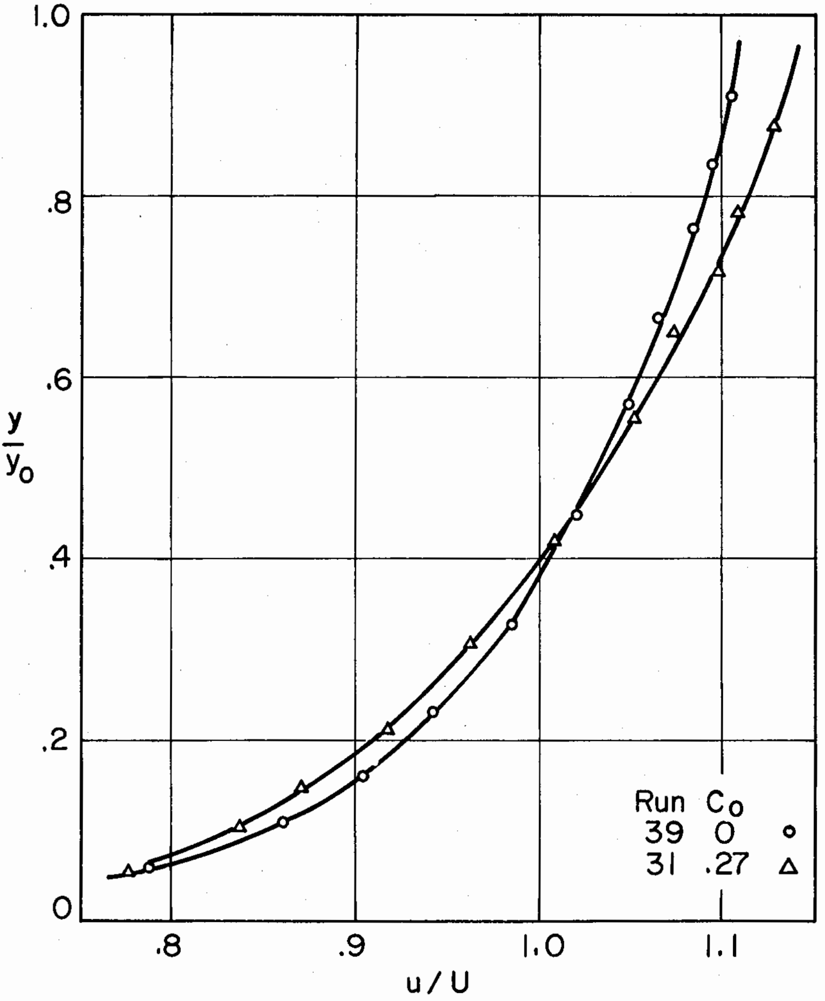

Fig. 1 Comparison of Velocity Profiles for Flows with and without Suspensions (Linear Plot). (Ref. 16)

equation (12)). In Figure 2 the variation of the effective viscosity with increasing concentration is given in accordance with equations (20) and (21) as confirmed by experiments in our laboratory [16].

Figure 3 shows the distribution of sediment over the depth in terms of absolute concentrations C in grams per liter for various values of Z, as presented in reference [16]. The experimental evidence clearly shows general agreement with the theory as long as the absolute concentrations C remain very small. When concentration distributions are plotted to logarithmic scale, Figure 3 shows that, in accordance with equations (16) and (18), the slopes of the concentration profiles with depth represent the exponents Z in the equations.

As has been pointed out, the correlation of the mean concentration C_m with the values of k obtained from various experiments cannot be satisfactory. But Vanoni and Nomicos [17] and Einstein and Chien [13] recognized that the higher concentrations near the boundary were largely responsible for the effect on k. A graph by Einstein and Chien showing the variation of k with a ratio of the power P_s to suspend the sediment in a vertical column of unit area to the power P_f to overcome the bottom resistance to flow in the unit area (i.e., $U \cdot \tau_o$), is given in Figure 4. The plot is noteworthy in view of the field and laboratory data included but the scatter, even for the laboratory data alone, is quite large. When Vanoni and Nomicos [17] analyzed their data for fine sand of .10 mm diameter in terms of the same power ratio, large scatter was again observed as seen in the upper part of Figure 5. However, when they concentrated the power to suspend particles to a layer only from 0.001 to .01 y_o near the bed given as P_s', the correlation of k with the power ratio P_s'/P_f is seen to improve substantially. It is felt that the latter approach succeeded somewhat better because the mean concentration in the thin bottom layer tended towards the maximum concentration C_o used in the analysis developed in equation (27). This approach fails, however, to account for the material reduction of k for near neutrally buoyant particles since for these the power P_s' would approach zero. It was successful in Figure 5 only because for all runs the specific gravity was that for sand.

When all experimental data of these investigators were extrapolated towards the bottom boundary, a maximum concentration C_o could be defined. The results of our laboratory tests with neutrally buoyant particles [16] as well as later tests by Ordonez [18] with sand were also analyzed to establish values of C_o for equation (27). Figure 6 shows the comparison of equation (27) with these experimental results relating the maximum concentrations C_o to the values of k as obtained from semi-logarithmic plots of u/U_* versus y/y_o. The agreement between the simple theory proposed in equation (27) and experimental results is quite satisfactory.

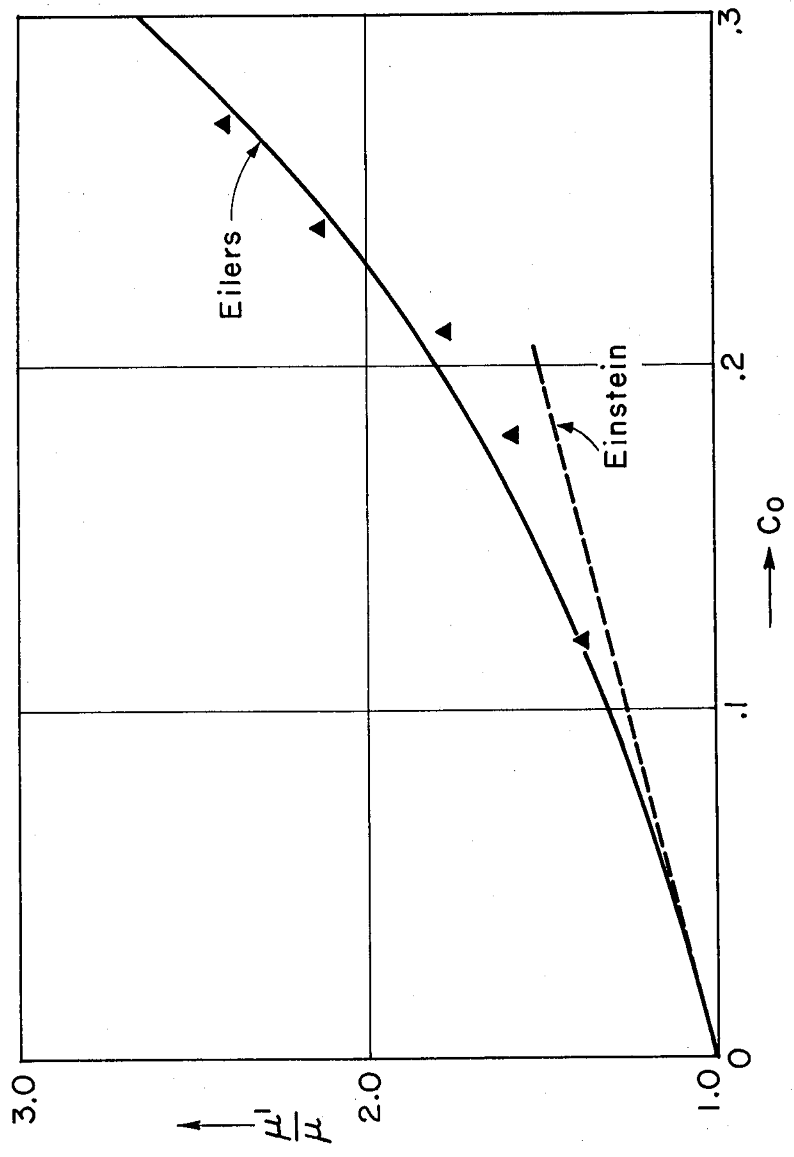

Fig. 2 Variation of Effective Viscosity μ' in Terms of Clear Water Viscosity μ with Volume Concentration Co. (Ref. 16)

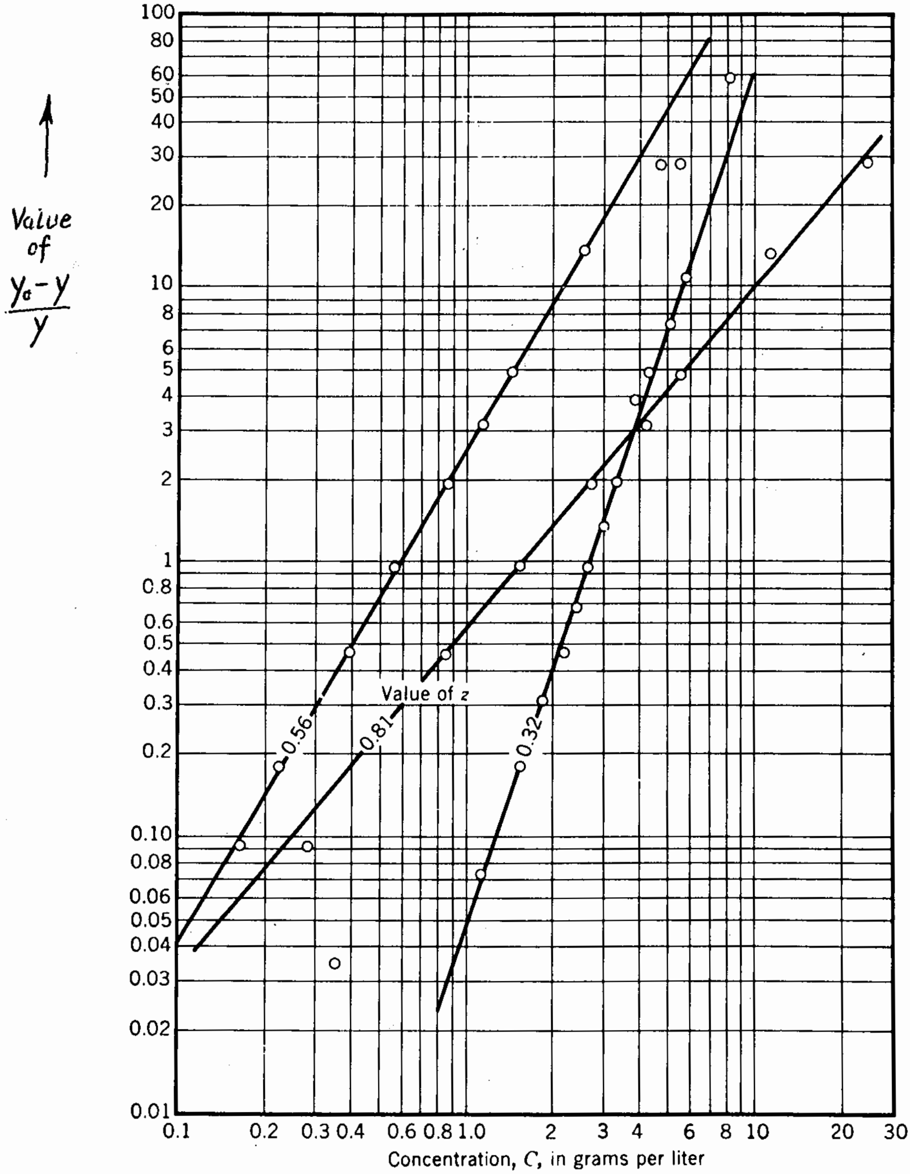

Fig. 3 Distribution of Sediment Concentration C over the Depth for Different Values of Exponent Z.(Ref. 1b)

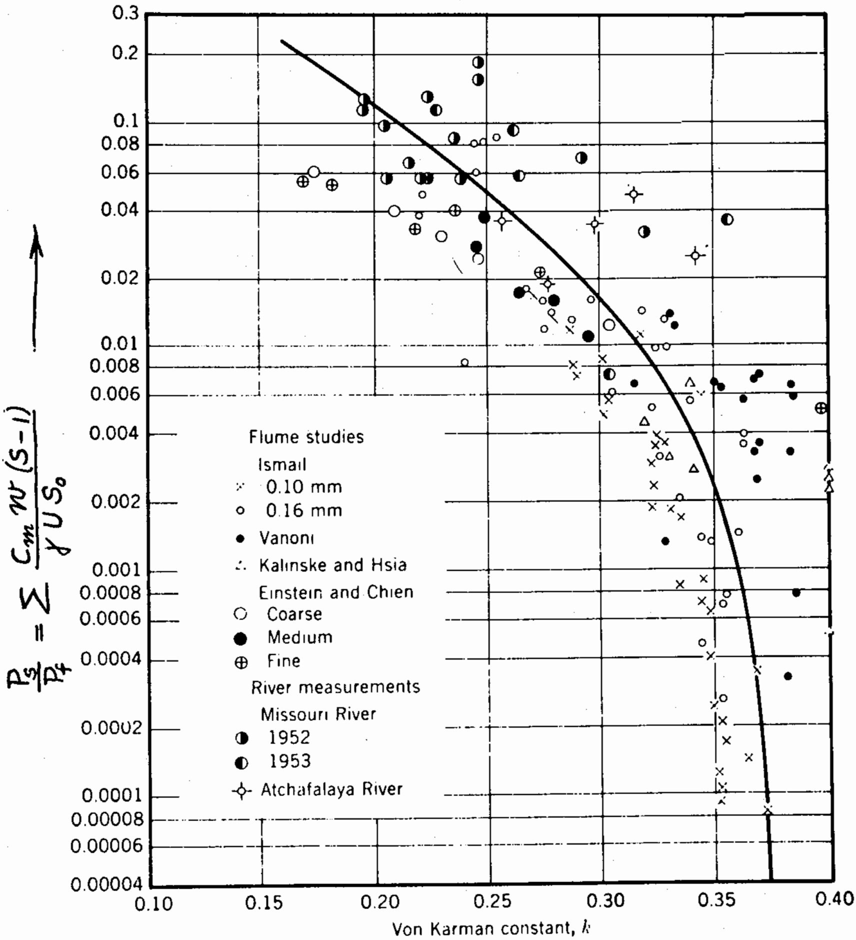

Fig. 4 Variation of k with Ratio of Power P_s to Suspend Particles to Power P_f to Overcome Bottom Resistance. (ref. 1b)

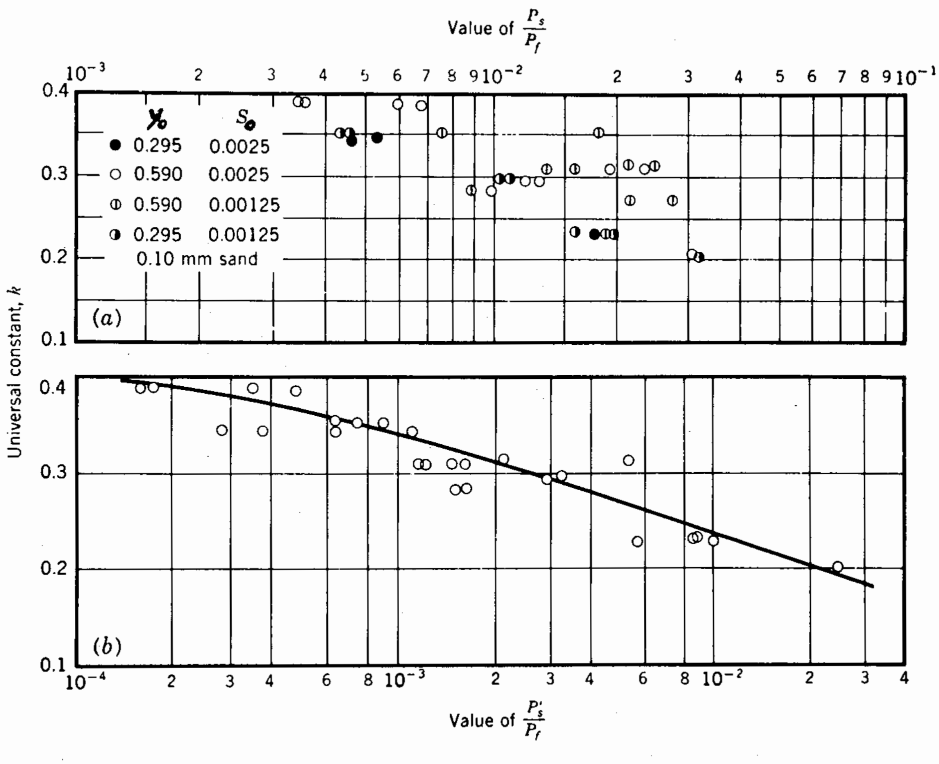

Fig. 5a Variation of k with Ratio of Power P_s to Suspend Particles to Power P_f to Overcome Bottom Resistance for Sand of .10 mm dia. and Various Flow Conditions. (Ref. 1b)

Fig. 5b The Same Data as in Figure 5a with P_s' Confined to Bottom Layer of .001 to .01 y_o.

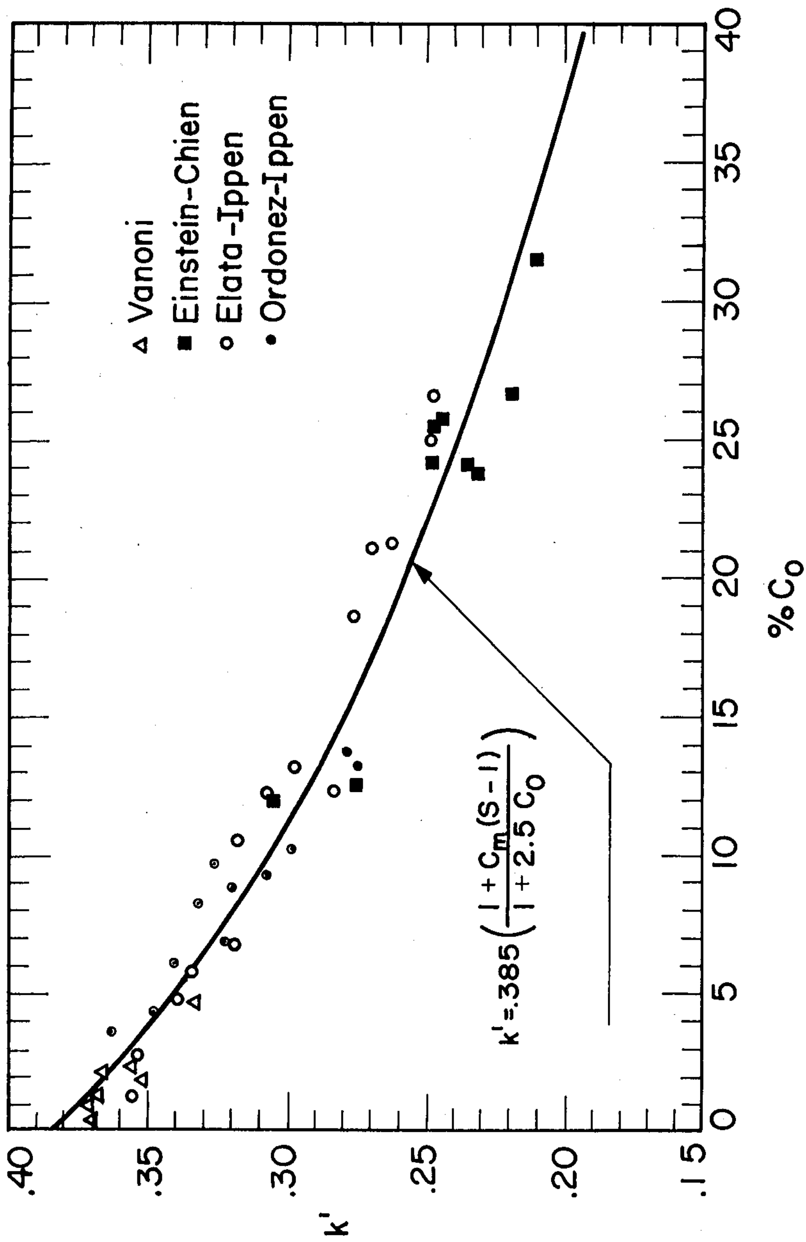

Fig. 6 Comparison of the Constant k′ as Defined by Equation (27) with Various Experimental Results. (ref. 10)

Velocity Distributions with Suspended Sediment

In the preceding section a relation was developed between the value of the coefficient aU_*/ν in the velocity distribution functions stated by equations (10) and (12) and the maximum sediment concentration C_o near the bed. With values of k' as determined for C_o, the velocity profiles over the upper portion of the stream can be described. In Figure 7 typical velocity distributions obtained by Einstein-Chien [13] for various concentrations of sand are seen, however, to exhibit a markedly different behavior from this upper portion particularly for the 10% of depth near the bottom. This departure from the linear condition of the semi-logarithmic law was analyzed for many similar data sets, and an essentially empirical correction in the velocity distribution equation was introduced by Ordonez [18] as follows:

$$\frac{u - U_{max}}{U_*} = \frac{1}{k'} \ell n \left(\frac{y}{y_o} - \psi \, \ell n \frac{y}{y_o}\right) \tag{28}$$

The term involving ψ representing a small depth ratio modifies the velocity distribution particularly in the critical region near the bed, as illustrated by Figure 8, for various values of ψ, which in most cases are of the order .001 to .016. For all runs in our laboratory as well as for those of Einstein-Chien and of Vanoni, experimental values of ψ were determined and good agreement was achieved between the function (28) and the measurements. The solid lines in Figure 8 represent the function (28) with the appropriate constant ψ for a number of laboratory experiments with different concentration distributions.

The next step was to establish a correlation between the sedimentation parameter Z in equations (17) and (19) which was evaluated from the experimental runs, the effective value of k' which depends primarily on the maximum concentration C_o, and the small factor ψ in equation (28). Figure 9 illustrates that such a correlation does exist as far as the four sets of experimental data obtained by different investigators for a wide variety of conditions can serve as evidence. In view of the difficult experimental evaluations, the correlation appears to be quite convincing, but additional work is in progress to establish further clarification.

Distribution of Sediment Concentrations

The major consequence of the modified velocity distribution equation (28) with regard to the distribution of suspended sediment is that equation (8) must be integrated anew with a local velocity gradient du/dy obtained as the derivative of equation (28). The effect of the sediment on the shearstress is usually very minor and is therefore neglected in the integration. The derivative of equation (28) is

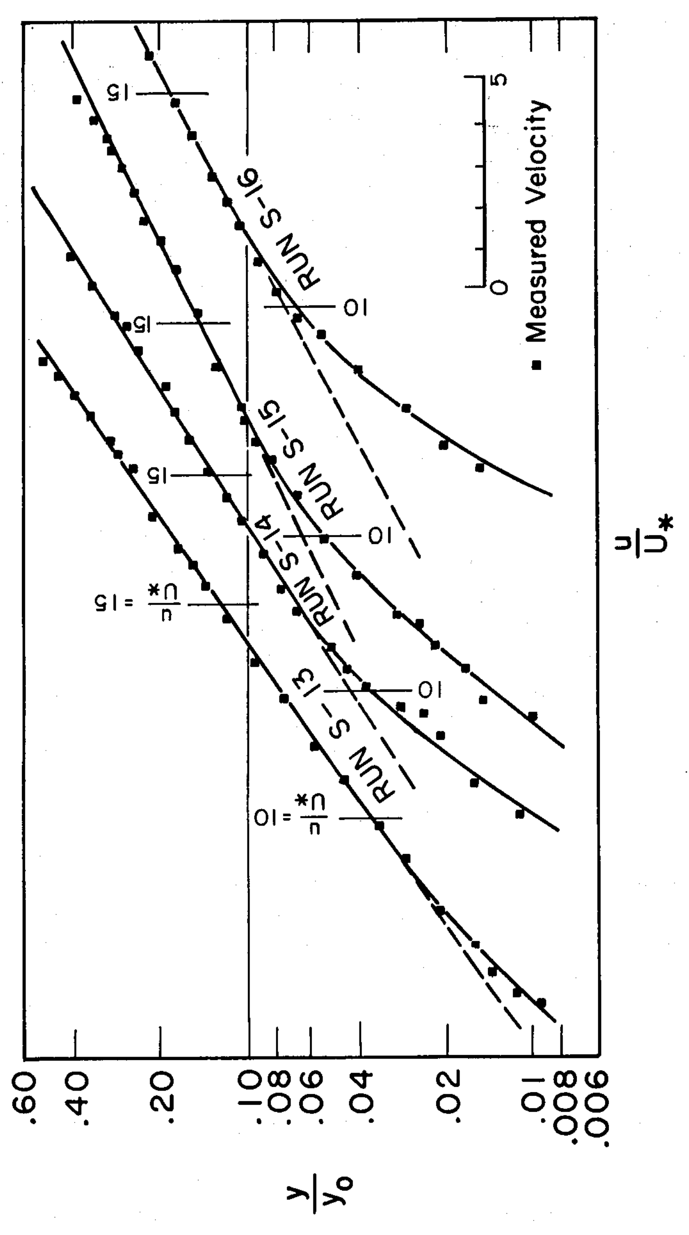

Fig. 7 Typical Velocity Distributions for Different Concentrations of Sand (Ref. 13)

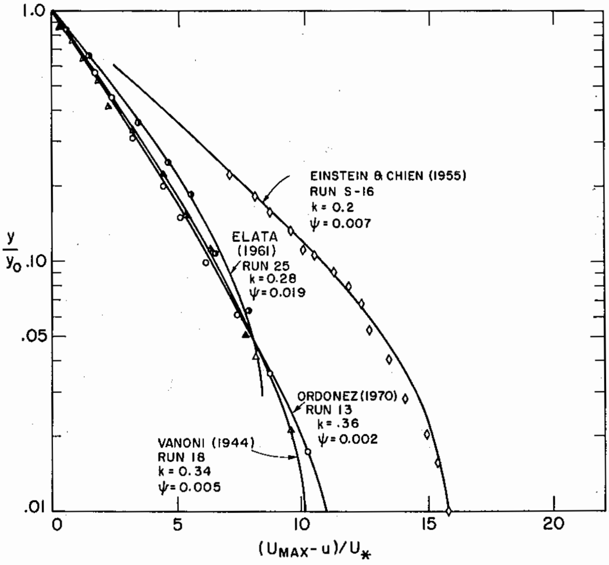

Fig. 8a Comparison of Experimental Velocity Distributions from Various Investigators with the Modified Velocity Distribution Equation (28).

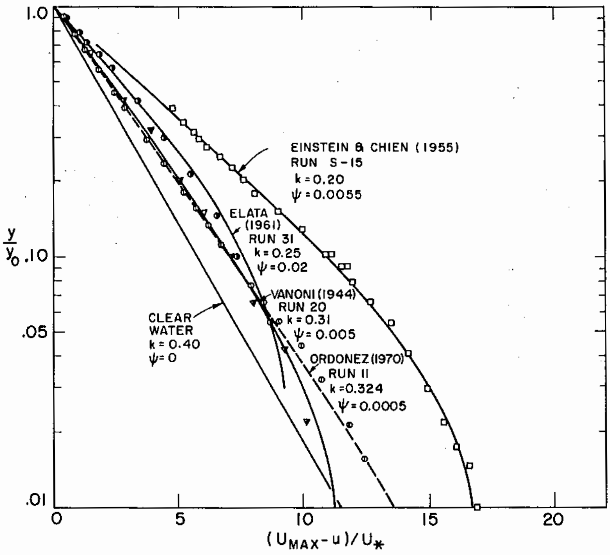

Fig. 8b Comparison of Experimental Velocity Distributions from Various Investigators with the Modified Velocity Distribution Equation (28)

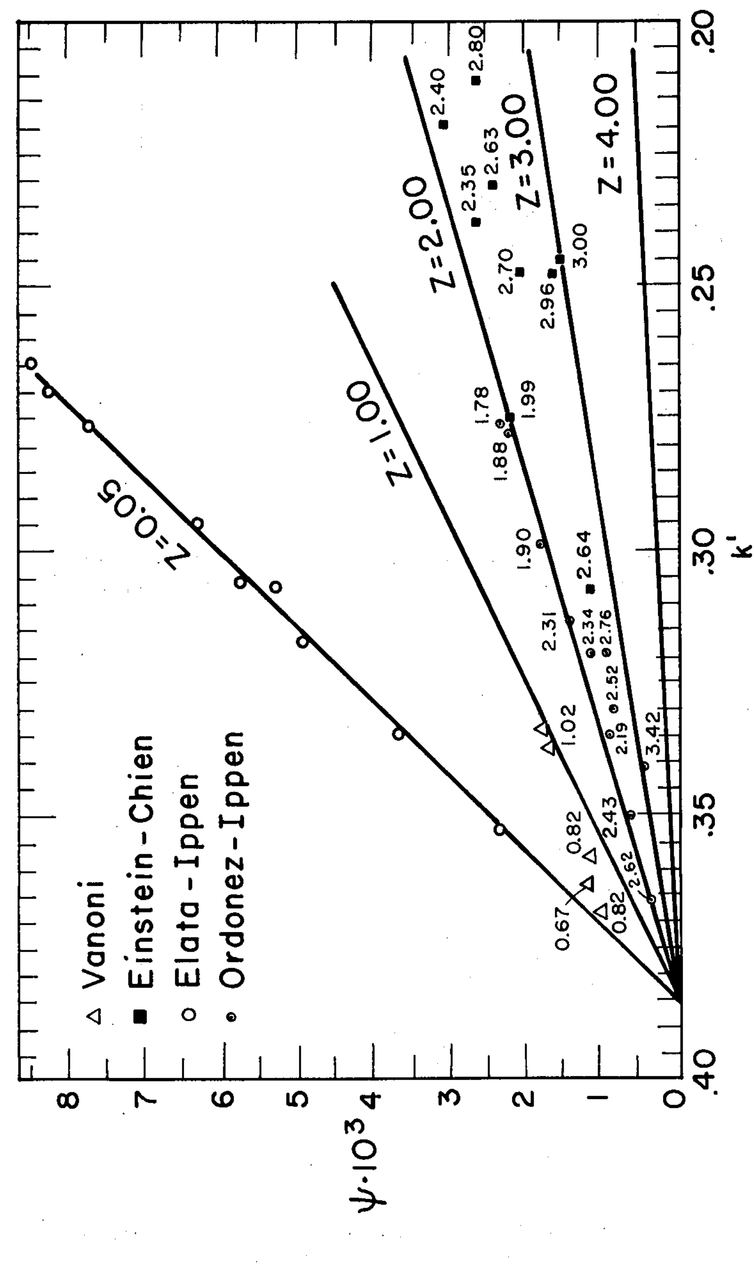

Fig. 9 Correlation between ψ and k′ for Different Values of Zexp

$$\frac{du}{dy} = \frac{U_*}{k'y} \frac{\frac{y}{y_o} - \psi}{\frac{y}{y_o} - \psi \ln \frac{y}{y_o}} \tag{29}$$

Introducing also the maximum concentration C_o near the bed as the reference concentration where $y/y_o = \psi$, the integration of equation (8) with equation (29) for the velocity gradient results in

$$\ln \frac{C}{C_o} = \frac{w}{k' U_*} \int_{\frac{y}{y_o}}^{\psi} \frac{\frac{y}{y_o} - \psi}{\frac{y}{y_o}(1 - \frac{y}{y_o})(\frac{y}{y_o} - \psi \ln \frac{y}{y_o})} d\left(\frac{y}{y_o}\right) \tag{30}$$

This equation was first given by Ordonez and Ippen [18] in 1970. The integral was evaluated by computer for a wide range of numerical values of ψ and $Z = w/k'U$ The function differs from the previous equations (16) and (18) by the introduction of k' from equation (27) and of the velocity gradient in accordance with equation (29). The former effect provides for a change in slope in a log-log plot of the sediment concentrations and the latter effect produces the increasing deviation from this slope particularly for the concentration distribution near the bed. This deviation from the exponential law is usually confined to the region below $y_o/10$.

Figure 10 reproduces several experimental data sets by Einstein and Chien [13]. These were obtained for rather large concentrations and are shown here for emphasis. When compared to the curves obtained by means of equation (30) they show generally good agreement. It is to be noted that the curves terminate at specific points near the bed where $y/y_o = \psi$ and $C = C_o$. It is clear that the maximum concentration C_o had to be determined by extrapolation of the experimental data to ψ and from equation (27) since measurements to this level are not available due to experimental difficulties. It may be surmised that ψ is more of a reference parameter than a physical quantity, as it was determined indirectly by recourse to measured velocity distributions

Many other experimental comparisons were made with comparable success [18]. Vanoni's experiments result in good agreement with both equations (18) and (30). This is due to his relatively low concentrations of fine sand (mean diameter d = .16 mm.), which extend only to within 5% of the depth near the bed. Einstein and Chien's measurements were carried out with mixtures of particles with D_{50} from .27 mm. to 1.30 mm. With the coarser particles the concentrations showed particularly the trends near the bed expressed by equation (30). The measurements also extended closer to the bottom boundary as shown in Figure 10.

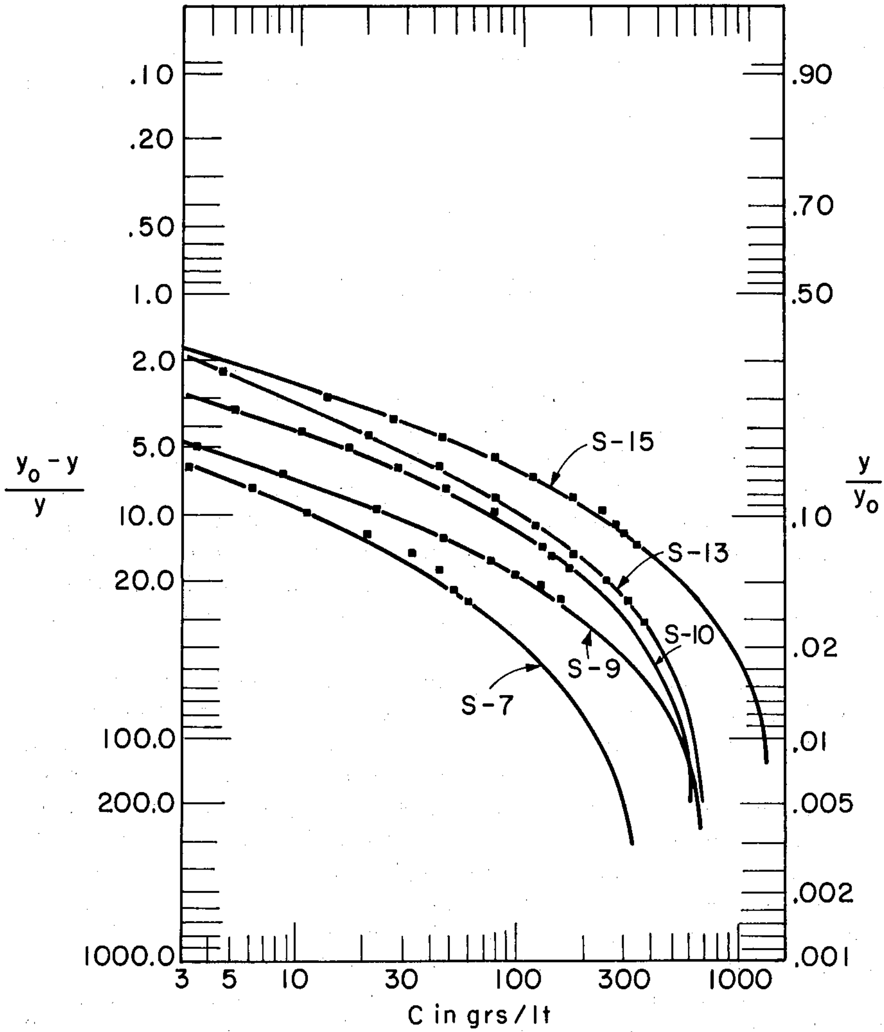

Fig. 10 Concentration Distributions C in Grams per Liter vs. Relative Depth, y/y_o (Einstein - Chien (13))

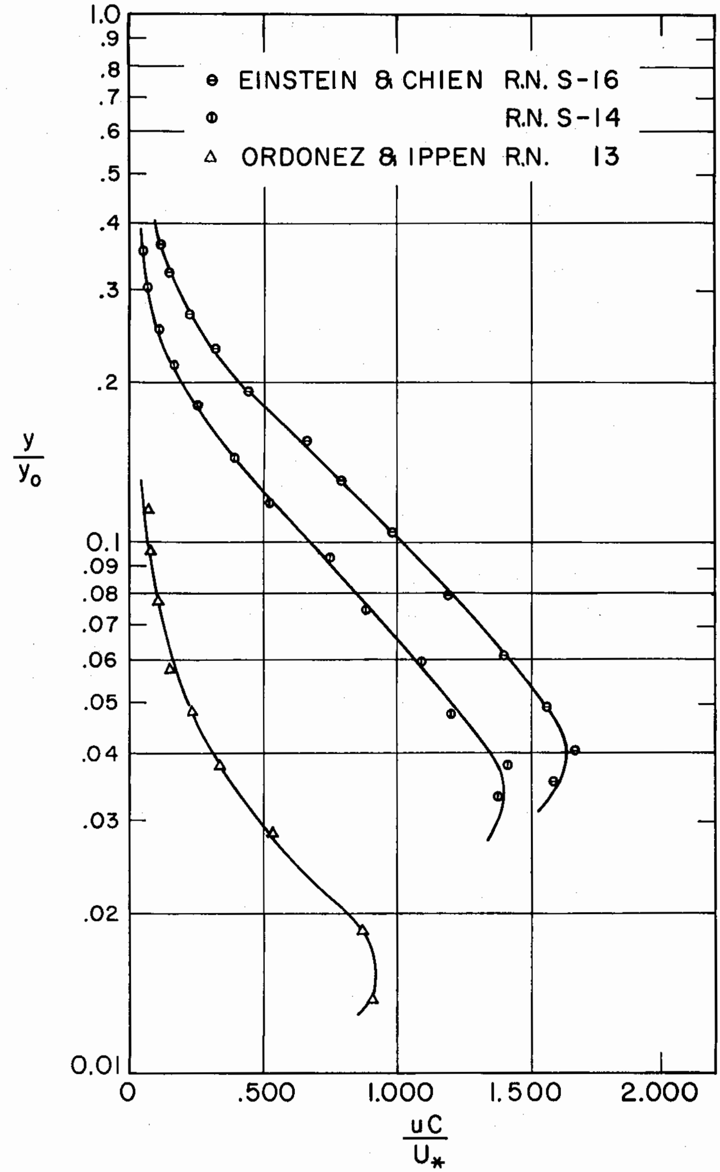

Fig. 11 Variation of Transport rates of Sediment uC/U_* over the Depth.

In the M.I.T. study by Ordonez and Ippen, fairly uniform Ottawa sand was used with a diameter D_{50} = .25 mm. However, the variation of the grain sizes from this mean contributed to some scatter. Measurements of concentrations were carried out to within .02 y/y_o near the bed.

Modifications of Hydraulic Parameters

Several interesting hydraulic aspects of flow with suspensions in contrast to clear water flow may be evaluated if the preceding relations are accepted as representing a satisfactory approach to the analysis of flow of suspensions. In accordance with the Darcy-Weisbach equation, the resistance coefficient is generally defined by:

$$\frac{U_*}{U} = \sqrt{\frac{f}{8}}. \tag{31}$$

Since the experimental evidence points to changing values of the Darcy-Weisbach resistance coefficient f for flow with suspensions, the mean velocity U must also change for a given shear velocity $U_* = \sqrt{g\, y_o\, S_o}$. By integrating equation (28) over the entire depth and dividing by y_o the relation between maximum velocity U_{max} and the mean velocity U is obtained as:

$$\frac{U_{max}}{U} = 1 + \frac{1}{k}\sqrt{\frac{f}{8}}\left[\frac{k}{k'}\int_1^{\psi} \ell n\left(\frac{y}{y_o} - \psi\, \ell n \frac{y}{y_o}\right) d\left(\frac{y}{y_o}\right)\right]. \tag{32}$$

For clear water flow with ψ = o and k/k' = 1 this reduces to:

$$\frac{U_{max}}{U} = 1 + \frac{1}{k}\sqrt{\frac{f}{8}} \tag{33}$$

The integral expression in equation (32) has been evaluated for the range of ψ from 0 to .016 to give a factor only 14% smaller than unity for the maximum ψ. The ratio k/k', however, may reach values of up to 2. The expression in brackets in equation (32) is therefore always larger than unity. Since all velocity profiles with suspended sediment show larger values of U_{max}/U than for clear water, it follows that the value in brackets in (32) must more than compensate for any possible decrease in f for a given shear velocity as explained for equation (31).

Table 1 gives a summary of basic data for a number of representative experimental runs selected from the four sets of references [12], [13], [16],

	1	2	3	4	5	6	7	8	9	10	11	12
Source of Data	S_o	y_o (ft)	U (fps)	U_{max} (fps)	f	U_* (fps)	k'	ψ	$\frac{U_{max}}{U}$ expt.	$\frac{U_{max}}{U}$ computed by Eq. 32	C_m vol. mean x 10^4	$\frac{U_{max} - U}{U_*}$
Vanoni (12)												
Run No. 1	0.0025	0.481	3.62	4.175	0.0236	0.197	0.375	0	1.151	1.146	0	2.67
18	0.00125	0.462	2.50	2.95	0.0235	0.136	0.31	0.005	1.181	1.163	4.42	3.013
20	0.0025	0.461	3.24	3.86	0.0283	0.193	0.34	0.005	1.190	1.161	7.05	2.747
Einstein-Chien [13]												
Run No. S-15	0.0262	0.408	10.00	12.80	0.0271	0.586	0.20	0.0055	1.28	1.269	250	4.648
S-16	0.0267	0.391	9.30	12.05	0.0310	0.580	0.20	0.007	1.295	1.281	293	4.568
Ordonez-Ippen [18]												
Run No. 11	0.005	0.291	5.89	6.55	0.0109	0.218	0.324	0.0005	1.110	1.114	21.0	3.044
13	0.005	0.335	5.20	5.86	0.0160	0.232	0.360	0.002	1.129	1.120	27.0	2.690
Elata-Ippen [16]												
Run No. 25	0	0.123	5.31	6.021	0.0157	0.237	0.28	0.019	1.131	1.132	1320	3.005
31	0	0.134	4.59	5.265	0.0154	0.202	0.25	0.020	1.148	1.147	2660	3.345

TABLE 1: Summary of Basic Data

[18]. They represent a large variety of hydraulic and concentration conditions. It is seen that the values of U_{max}/U computed from equation (32) compare very favorably with the experimental values. They could not have been obtained from the equation (33) for clear water.

It has been observed that the resistance coefficient f may decrease or increase with increasing sediment concentrations. This problem is as yet not resolved clearly, but equations (31) and (32) provide at least further insight into this aspect.

Many of the conclusions with regard to the dependence of the hydraulic parameters on sediment concentrations are independently confirmed by the contributions to this field of M. Hino [19), who developed the hydrodynamic theory of flow of suspensions on the basis of energy dissipation in the flow including suspended particles and total energy production.

Evaluation of Total Transport

With the velocity distribution defined by equation (28) and the distribution of volume concentration given by equation (30), the distribution of the sediment transport rate over the depth can be determined. Such distributions are given for illustration in Figure 11 for three cases as indicated. The volume rate of transport is given in dimensionless form as uC/U_* and plotted against y/y_o. The logarithmic scale for y/y_o emphasizes the predominance of sediment flux in the lower 10 to 20% of the depth.

From these plots the total sediment flux can be obtained by integration which was done numerically using the relation

$$\alpha\, U\, y_o\, C_m = \int_0^{y_o} u\ C\ dy \qquad (34)$$

wherein the mean concentration

$$C_m = \frac{1}{y_o} \int_0^{y_o} C\ dy \qquad (35)$$

The factor α by which the mean concentration C_m as defined by the expression (35) is multiplied in equation (34) represents a correction factor to obtain the true mean concentration C_m' from the integration of the local transport rates over the depth. In Table 2 a few such evaluations of α have been made from available data. The more uniform the distribution of sediment, the closer is the value of α to unity, as is obvious for the nearly neutrally buoyant particles of the Elata-Ippen runs.

Source of Data	Run No.	$C_m \times 10^2$	$C_m' \times 10^2$	α
Elata-Ippen [16]	31	26.6	26.6	1.00
Vanoni [12]	20	.071	.067	.945
Ordonez-Ippen [18]	13	.27	.185	.686
Einstein-Chien [13]	14	1.38	.77	.557
	16	2.93	1.48	.505

TABLE 2

The value of α for various conditions of sediment transport can be predicted only through the integration of the product of velocity (equation (28)) and concentration (equation (30)) over the depths. Such evaluations are quite complex and only possible by computer. No simple correlations are possible since the variations of α depend on the interdependent functions for velocity and sediment distribution. The values of α given in Table 2, however, show that actual concentrations C_m' differ materially from the arithmetic average concentration C_m obtained from suspended sediment concentration surveys.

Conclusions and Summary

The study presented in its essential phases is part of a comprehensive investigation into the characteristics of flow with solid suspensions at MIT. The preceding sections dealt with analytical and experimental phases of this study pertaining to two-dimensional steady and uniform flow over a smooth boundary with particle suspensions in various concentrations.

It was shown that the variation of the Von Karman constant k′ is primarily a function of the maximum concentrations of sediment C_o.

A velocity distribution function is given which depends on the shear velocity, the value of k′, and a parameter ψ. The value of ψ is related to k′ and C_o.

The concentration distribution has been redeveloped with the modified velocity distribution function and evaluated. The total suspended load for individual particle sizes may be determined from the mean concentration and, therefore, also the transport rate of suspended sediment for the two-dimensional case.

The effects of the suspensions on the mean velocity, maximum velocity, and resistance coefficient have been shown to be consistent with experimental observations and the analytical approaches employed.

The general problem of transport of sediments in turbulent streams is still unsolved, but important insights have been gained in recent years, and the results of the MIT research in this field hopefully have contributed to this advance in our knowledge. It is an important area of research in the present era of concern with our water environment, and therefore merits further attention and support in analytical, experimental and field explorations.

Acknowledgements

Much of the introductory material presented was taken from the professional literature and is acknowledged in the list of references. A part of the analytical approach originated from unpublished notes of the writer. Special recognition, however, is recorded here to Dr. Nelson A. Ordonez-C., of Lima, Peru, who carried out his doctoral work in this area of suspended sediment transport at the Ralph M. Parsons Laboratory for Water Resources and Hydrodynamics in the Civil Engineering Department of MIT in the years 1968-1970 under the supervision of the author. Many of the figures, experiments, and analytical evaluations cited in the text originated through his efforts. Grateful acknowledgment is due also to Mr. Sergio Montes, Research Assistant in the same laboratory, for his extensive assistance on many details of the material prepared for the final draft of this paper.

REFERENCES

1. "Sediment Transportation Mechanics," Progress Reports of Task Committee on Sedimentation of the Hydr. Div. of the ASCE.
   1a. "Initiation of Motion," *Proc. A.S.C.E.*, Vol. 92, No. HY2, 1966; also "Sediment Discharge Formulas," *Proc. A.S.C.E.*, Vol. 97, No. HY4, 1971.
   1b. "Suspension of Sediment," *Proc. A.S.C.E.*, Vol. 89, No. HY5, 1963.
2. Graf, Walter H., *Hydraulics of Sediment Transport*, McGraw-Hill Book Co., New York, 1970.
3. Shields, A., "Anwendung der Aehnlichkeitsmechanik und Turbulenzforschung auf die Geschiebebewegung," Mitteil. Preuss. Versuchsanstalt fuer Wasser, Erd, und Schiffsbau, Berlin, No. 26, 1936.
4. Kennedy, John F., "The Mechanics of Dunes and Antidunes in Erodible Bed Channels," Journal of Fluid Mechanics, Vol. 16/4, 1963.
5. O'Brien, M. P., "Review of the Theory of Turbulent Flow and Its Relation to Sediment Transport," *Trans. American Geophysical Union*, 1933.
6. Schmidt, W., "Der Massenaustausch in Freier Luft Und Verwandte Erscheinungen," *Probleme der Kosmischen Physik*, Vol. 7, Hamburg, 1925.
7. Hurst, H. E., "The Suspension of Sand in Water," *Proc.*, Royal Society, London, Series A. Vol. 157, 1929.
8. Rouse, H., "Experiments on the Mechanics of Sediment Suspension," *Proc. Fifth International Congress of Applied Mechanics*, Cambridge, Mass., 1938.
9. Krey, H., "Die Quergeschwindigkeitskurve bei Turbulenter Stroemung," *Zeitschrift fuer Ang. Mathematik und Mechanik*, Vol. 7, No. 2, 1927.
10. Ippen, A. T., "Transport of Solids by Turbulent Flow in Channels and Conduits," IUTAM Symposium on Flow of Fluid-Solid Mixtures, Cambridge, England, 1969 (unpublished invited lecture).
11. Rouse, H., "Modern Conceptions of the Mechanics of Turbulence," *Trans. A.S.C.E.*, Vol. 102, 1937.
12. Vanoni, Vito A., "Transportation of Suspended Sediment by Water," *Trans. A.S.C.E.*, Vol. 111, 1946.
13. Einstein, H. A., and Chien, N., "Effects of Heavy Sediment Concentration Near the Bed on Velocity and Sediment Distribution," University of California, Inst. of Eng. Research, No. 8, 1955.
14. Einstein, H. A., *Annalen der Physik*, Vol. 19, p. 286, 1906 and Vol. 34, p. 591, 1911.
15. Eilers, H., "Die Viskositaet von Emulsionen Hochviskoser Stoffe als Funktion der Konzentrationen," *Kolloid-Zeitschrift*, Vol. 97, p. 313, 1941.
16. Elata, C., and Ippen, A. T., "The Dynamics of Open Channel Flow with Suspensions of Neutrally Buoyant Particles," M.I.T., Hydrodynamics Laboratory, Techn. Report No. 45, 1961.
17. Vanoni, V. A., and Nomicos, G. N., "Resistance Properties of Sediment-Laden Streams," *Trans. A.S.C.E.*, Vol. 125-I, 1960.
18. Ordonez-C., Nelson A., "The Absolute Concentration Distribution of Suspended Sediment in Turbulent Streams," Ph.D. Thesis, M.I.T., R. M. Parsons Lab. for Water Resources and Hydrodynamics, July 1970.
19. Hino, Mikio, "Turbulent Flow with Suspended Particles," *Proc. A.S.C.E.*, Vol. 89, No. HY4, 1963.

TABLE OF NOTATIONS

Roman Letters

a	small distance from bottom defined by equation (10)
b	arbitrary reference distance from bottom
c or C	local concentration of sediment
C_o	maximum sediment concentration
C_m	average sediment concentration
d or D	mean particle diameter
f	Darcy-Weisbach resistance coefficient
$f(\ )$	function of ( )
F	Froude number of flow
g	acceleration of gravity
k	Von Karman universal constant
k'	effective constant for velocity distributions with sediment
P_s	power to suspend sediment particles per unit area
P_f	power to overcome bottom resistance per unit area
q	discharge per unit width
q_s	sediment transport rate per unit width
S	specific gravity of sediment
S_o	slope of bottom or energy gradient
u	local velocity
U	average velocity for cross-section
U_*	shear velocity $\sqrt{\tau_o/\rho}$
U_{max}	maximum velocity at surface
w	settling velocity of particles in still water
x	distance in direction of flow
y	local depth measured from bottom
y_o	total depth of stream
Z	sedimentation parameter as defined by equations (17) and (19)

Greek Letters

α	=	proportionality factor used as defined locally
β	=	ratio of mass exchange coefficient to momentum transfer coefficient
γ	=	specific weight
δ'	=	thickness of laminar sublayer
ϵ_m	=	turbulent momentum transfer coefficient
ϵ_s	=	kinematic mass exchange coefficient
μ	=	dynamic viscosity
μ'	=	dynamic viscosity for fluid-particle mixtures
ν	=	kinematic viscosity = μ/ρ
ρ	=	density = γ/g
τ	=	local shear stress
τ_0	=	maximum shear stress at bottom
ψ	=	small experimental factor in equation (28)

BEAMS ON ONE-WAY ELASTIC FOUNDATIONS

by

K.K. LIN,[1] S.E. SWARTZ,[2]
W.W. WILLIAMS[3]

Introduction

Mat foundations under certain structures, such as silos, water-storage tanks, coal-storage towers, and footing foundations supporting a group of columns, are frequently designed and constructed in the form of beams resting on soil. The theory of bending of beams on elastic foundations, developed by Winkler (1)[4], is based on the assumption that the intensity of the continuously distributed reaction of the foundation at every point is proportional to the deflection at that point. Its application to the design of foundations has received considerable attention. Other methods of analysis have been proposed by Hetenyi (2), Biot (3), Vesić (4), Levinton (5), Malter (6), Bowles (7), and Matlock (8). One common feature of these works is that the foundation can support a tensile stress. Recently, Tsai and Westmann (9) have indicated an approach based on a tensionless foundation assumption to account for the effects of beam uplift. A simplified procedure for the solution of the beam-foundation problem for the case of tensionless soil will be presented.

Problem Formulation

In the classical solution for beams on foundations, it is usual to assume that foundation properties are identical in tension and compression. Often the resulting analysis then indicates an alternating reaction, thus implying that the foundation can support a tensile stress. Usually this is not an acceptable result for real soil. Therefore, the Winkler model is modified to take into account the effect of beam uplift which then leads to a non-linear solution (9). As the beam is supported along its entire length by an elastic medium, which may or may not be continuous, the problem formulation and solution can be made by assuming that the beam rests on "one-way", equally spaced, elastic springs. The springs may be spaced in such a way and have the appropriate stiffnesses such that they adequately represent the soil medium. The subgrade tensile stress in the uplift portion of beam can be relaxed simply by setting the spring constants of those portions equal to zero.

[1] Engineer, New Rochelle, New York
[2] Assistant Professor, Kansas State University, Manhattan, Kansas
[3] Associate Professor, Kansas State University, Manhattan, Kansas
[4] Numerals in parentheses refer to corresponding items in Appendix I – References

Elastic solutions of beam-foundation problems are based on the assumption that the soil behaves as an elastic, homogeneous, infinite, and isotropic solid, defined by a modulus of deformation, E_s, and a Poisson's ratio, ν. It is further assumed that there are no shearing stresses at the contact interface between beam and soil. If the problem is so posed, Winkler's model can be replaced by a continuous beam resting on a set of springs each with stiffness constant K (10). This stiffness is defined by

$$K = K_s' \, a$$

where

$K_s' = K_s \, B$ = modulus of subgrade reaction x width of beam.

a = cell length (distance between springs equally spaced).

The solution of this problem then can be expressed by a matrix formulation as follows (11). Consider a beam supported by equally spaced springs, shown in Fig. 1, where γ is the uniform dead load, and Q is a concentrated load. In the following, each spring support point on the beam is considered to be a joint.

Load Matrix (P) and Displacement Matrix (X)

The joint load matrix [P] is defined as a column vector whose elements are the applied joint loads with the joints fixed. The displacement matrix [X] consists of the final displacements at the joints measured in the same directions as the loads. Referring to Fig. 2, the load matrix [P] is expressed by

$$[P] = \begin{bmatrix} P_1 \\ P_2 \\ \cdot \\ \cdot \\ \cdot \\ P_{n_c+1} \\ \hdashline P_{n_c+2} \\ P_{n_c+3} \\ \cdot \\ \cdot \\ \cdot \\ P_{2n_c+2} \end{bmatrix} \begin{matrix} \left.\vphantom{\begin{matrix} a\\a\\a\\a\\a\\a \end{matrix}}\right\} \text{moment terms} \\ \text{-----------------------} \\ \left.\vphantom{\begin{matrix} a\\a\\a\\a\\a\\a \end{matrix}}\right\} \text{force terms} \end{matrix} \qquad (1)$$

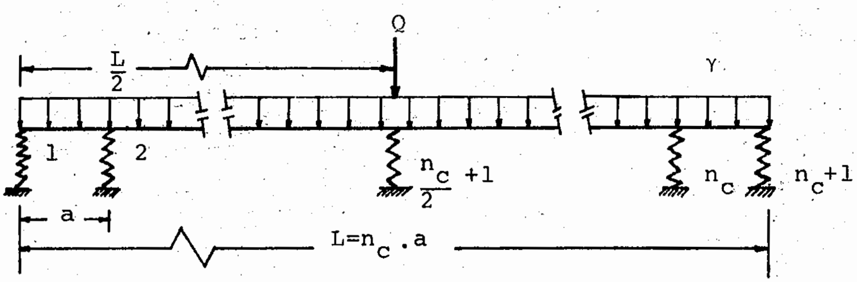

Fig. 1 Beam on Equally Spaced Spring Supports

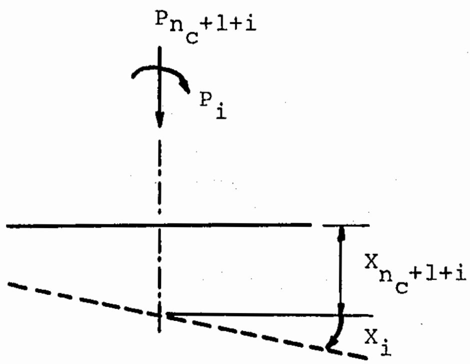

Fig. 2 Fixed Edge Forces and Final Deflections at ith Joint

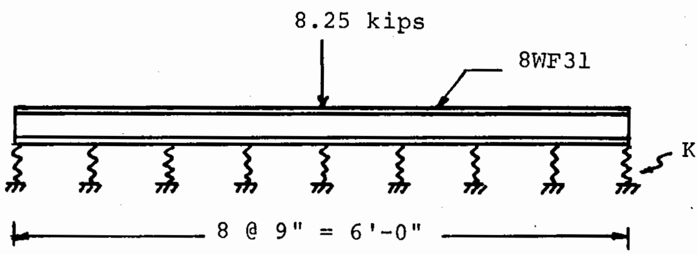

Fig. 3 Example 1. Beam tested by Vesić (4)

and the displacement matrix [X] is expressed by

$$[X] = \begin{bmatrix} X_1 \\ X_2 \\ \cdot \\ \cdot \\ \cdot \\ X_{n_c+1} \\ \text{------} \\ X_{n_c+2} \\ X_{n_c+3} \\ \cdot \\ \cdot \\ \cdot \\ X_{2n_c+2} \end{bmatrix} \begin{matrix} \left.\begin{matrix} \\ \\ \\ \\ \\ \\ \end{matrix}\right\} \text{rotation terms} \\ \text{----------------} \\ \left.\begin{matrix} \\ \\ \\ \\ \\ \\ \end{matrix}\right\} \text{displacement terms} \end{matrix} \qquad (2)$$

These forces and displacements are related by (11):

$$[P]_{NP} = [ASA^T]_{NP \times NP}[X]_{NP} \cdots\cdots\cdots\cdots \quad (3)$$

In the above, NP = $2n_c + 2$. (A) relates joint forces to member and spring forces and is (11)

$$[A] = \left[\begin{array}{c|c} A_1 & A_2 \\ \hline A_3 & A_4 \end{array}\right], \ (2n_c+2) \times (3n_c+1)$$

and

$$[A_1] = \begin{bmatrix} 1 & 0 & 0 & 0 & \cdot\cdot\cdot & 0 & 0 & 0 \\ 0 & 1 & 1 & 0 & \cdot\cdot\cdot & 0 & 0 & 0 \\ \cdot & & & & & & & \cdot \\ \cdot & & & & & & & \cdot \\ \cdot & & & & & & & \cdot \\ 0 & 0 & 0 & 0 & \cdot\cdot\cdot & 1 & 1 & 0 \\ 0 & 0 & 0 & 0 & \cdot\cdot\cdot & 0 & 0 & 1 \end{bmatrix}, \ (n_c + 1) \times (2n_c)$$

$[A_2] = [0], \ (n_c+1) \times (n_c+1)$

$$[A_3]\begin{bmatrix} 1/a & 1/a & 0 & 0 & 0 & 0 & . & . & . & 0 & 0 & 0 & 0 \\ -1/a & -1/a & 1/a & 1/a & 0 & 0 & . & . & . & 0 & 0 & 0 & 0 \\ 0 & 0 & -1/a & -1/a & 1/a & 1/a & . & . & . & 0 & 0 & 0 & 0 \\ . & & & & & & & & & & & & . \\ . & & & & & & & & & & & & . \\ . & & & & & & & & & & & & . \\ 0 & 0 & 0 & 0 & 0 & 0 & . & . & . & -1/a & -1/a & 1/a & 1/a \\ 0 & 0 & 0 & 0 & 0 & 0 & . & . & . & 0 & 0 & -1/a & -1/a \end{bmatrix}$$

$(n_c + 1) \times (2n_c)$

$$[A_4] = \begin{bmatrix} -1 & & & & & 0 \\ & -1 & & & & \\ & & -1 & & & \\ & & & . & & \\ 0 & & & & . & \\ & & & & & . \end{bmatrix}, \quad (n_c + 1) \times (n_c + 1)$$

[S] is the structure stiffness matrix and is given by (11)

$$[S] = \left[\begin{array}{c|c} S_1 & S_2 \\ \hline S_3 & S_4 \end{array}\right], \quad (3n_c + 1) \times (3n_c + 1)$$

$$\begin{bmatrix} \frac{4EI}{a} & \frac{2EI}{a} & 0 & 0 & . & . & . & 0 & 0 \\ \frac{2EI}{a} & \frac{4EI}{a} & 0 & 0 & . & . & . & 0 & 0 \\ 0 & 0 & \frac{4EI}{a} & \frac{2EI}{a} & . & . & . & 0 & 0 \\ 0 & 0 & \frac{2EI}{a} & \frac{4EI}{a} & . & . & . & 0 & 0 \\ 0 & 0 & 0 & 0 & . & . & . & \frac{4EI}{a} & \frac{2EI}{a} \\ 0 & 0 & 0 & 0 & . & . & . & \frac{2EI}{a} & \frac{4EI}{a} \end{bmatrix}$$

$(2n_c) \times (2n_c)$

$$[S_2] = [S_3] = (n_c + 1) \times (n_c + 1)$$

$$[S_4] = \begin{bmatrix} K & & & & \\ & K & & & \\ & & \cdot & & 0 \\ & & & \cdot & \\ & 0 & & & K \end{bmatrix} \qquad (n_c + 1) \times (n_c + 1)$$

In the above, EI is the flexural stiffness of the beam.

From (3),

$$[X] = [ASA^T]^{-1} [P] \qquad \ldots\ldots\ldots\ldots\ldots\ldots \quad (4)$$

After the spring deformations have been determined from equation (4), the spring forces may be obtained by

$$F_i = K\, X_{n_c + 1 + i} \qquad \ldots\ldots\ldots\ldots\ldots\ldots\ldots \quad (5)$$

in which F_i is the force in the ith spring and X_{n_c+1+i} is the deflection in the ith spring.

In applying the above procedure to the problem of a beam on a tensionless foundation, an iterative technique is used. Deflections are first calculated as though the springs can take tension. For those points wherein the beam deflects upward the spring constants are set equal to zero in the $[S^4]$ matrix and new deflections are determined. The solution generally converges within two or three cycles. A computer program written in FORTRAN IV was used to perform the numerical calculations.

This program is a modification of one given by Wang (11) and is efficient and fairly compact. It may be readily adopted as a subroutine in a larger program. The program was executed on the IBM 360-50 computer at the KSU Computation Center but may be easily modified to run on smaller computers such as the IBM 1620 or 1130. The program – source deck, listing and sample problem – may be obtained from the authors.

Numerical Examples

Example 1.

A short beam (Fig. 3) which has its unit weight included in the analysis for the purpose of a comparison with results given from a soil test by Vesić (4).

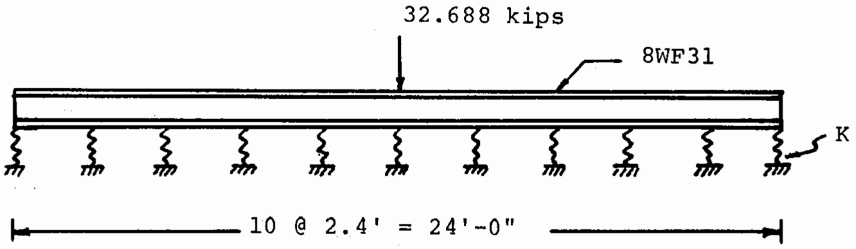

Fig. 4 Example 2A. Short Beam Comparison with Bowles Finite and Infinite Beam Analysis (7)

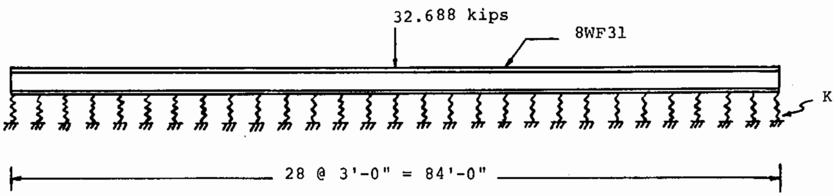

Fig. 5 Example 2B. Long Beam Comparison with Bowles Infinite Beam Analysis (7)

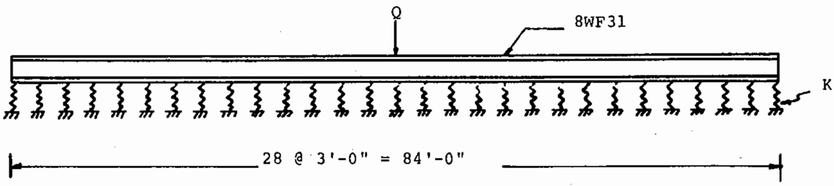

Fig. 6 Example 3. Long Beam Comparison with Infinite Beam Analysis of Tsai and Westmann (9) for Q = 8.6 kips, 12.9 kips, 17.2 kips, 34.4 kips

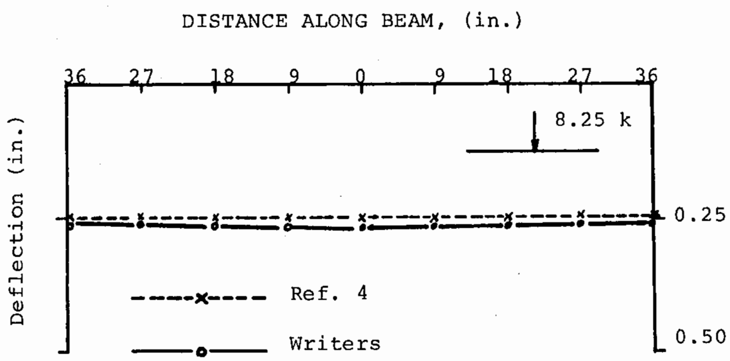

Fig. 7 Comparison with Soil Test Results (4) for Example 1

Beam length L = 72 in., center load Q = 8250 lb., unit weight γ = 31 lb./ft., spring constant K = 49 kip/ft. Cross section properties of the beam and subgrade are shown in Tables I and II. The results are shown in Fig. 7.

Table I – Data on Beam Section Used in Examples

Beam	Width B inches	Depth inches	Area Sq. in.	Moment Inertia I $inch^4$	Modulus of Elasticity E; psi
8WF31	8.0	8.0	9.12	109.7	30 x 10^5

Table II – Properties of Micaceous Silt Subgrade Used in Examples

Modulus of Elasticity of Soil Es, psi	Poisson's Ratio "‖"	Modulus of Subgrade Reaction Ks, psi
1192	0.25	454

Example 2.

Case A – A short beam with the same cross-section properties as in Example 1 but with unit weight not included in the analysis (Fig. 4). The results are compared with Bowles finite and infinite beam solutions (7) and plotted in Fig. 8. L = 2.4 ft., Q = 32.688 kips, K = 156.8 kip/ft.

Case B – The same beam as in Case A but longer and with the unit weight not included in the analysis (Fig. 5). The results are compared with Bowles infinite solution (7) and plotted in Fig. 9. L = 84 ft., Q = 32.688 kips, a = 3 ft., K = 196 kip/ft.

Example 3.

A long beam with the same cross-section as in Example 1 and with unit weight included in the analysis (Fig. 6). As the problem of the tensionless foundation is of prime interest, attention has been concentrated on solutions for the 8WF31 steel beam resting on a micaceous silt subgrade subjected to center loads of 8.6 kips, 12.9 kips, 17.2 kips, and 34.4 kips. This corresponds to the cases of n = 1.0, 1.5, 2.0, 4.0 discussed by Tsai (9). The results which are compared to his tensionless foundation solutions are shown in Figs. 10 to 13. Other parameters used in this example are L = 84 ft., a = 3 ft., γ = 31 lb./ft., K = 196 kip/ft.

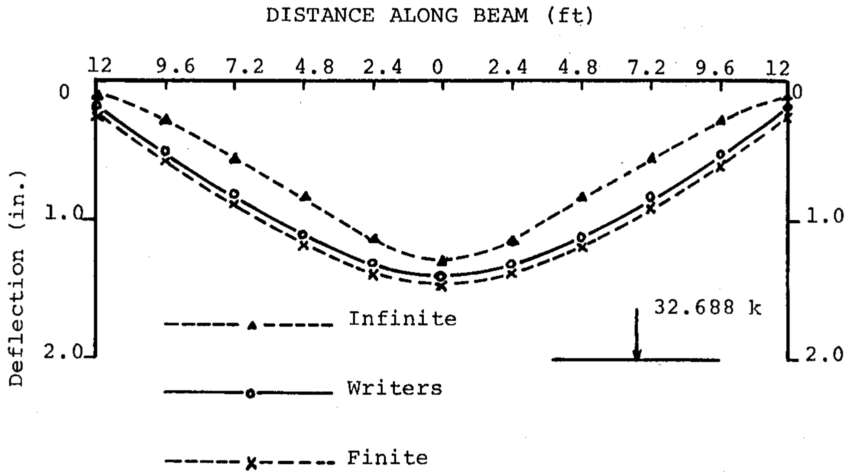

Fig. 8 Comparison of Deflections with Bowles (7) Finite and Infinite Beam Solution for Example 2A

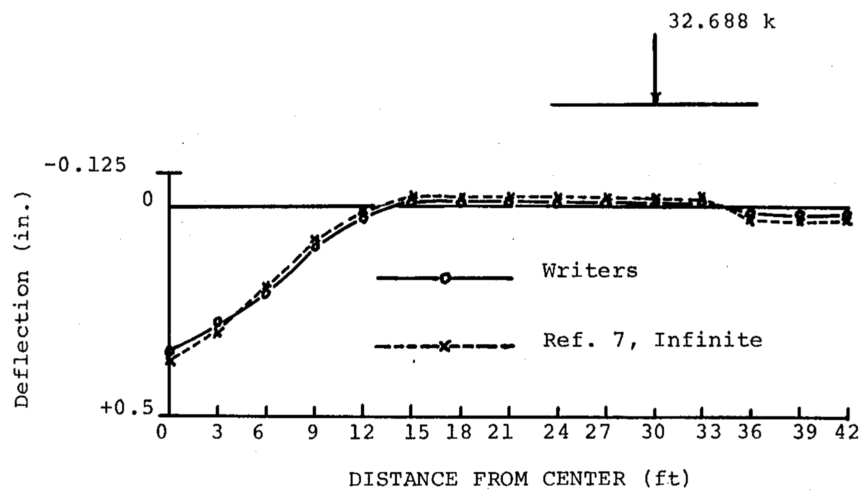

Fig. 9 Comparison of Deflections with Bowles (7) Infinite Beam Solution for Example 2B

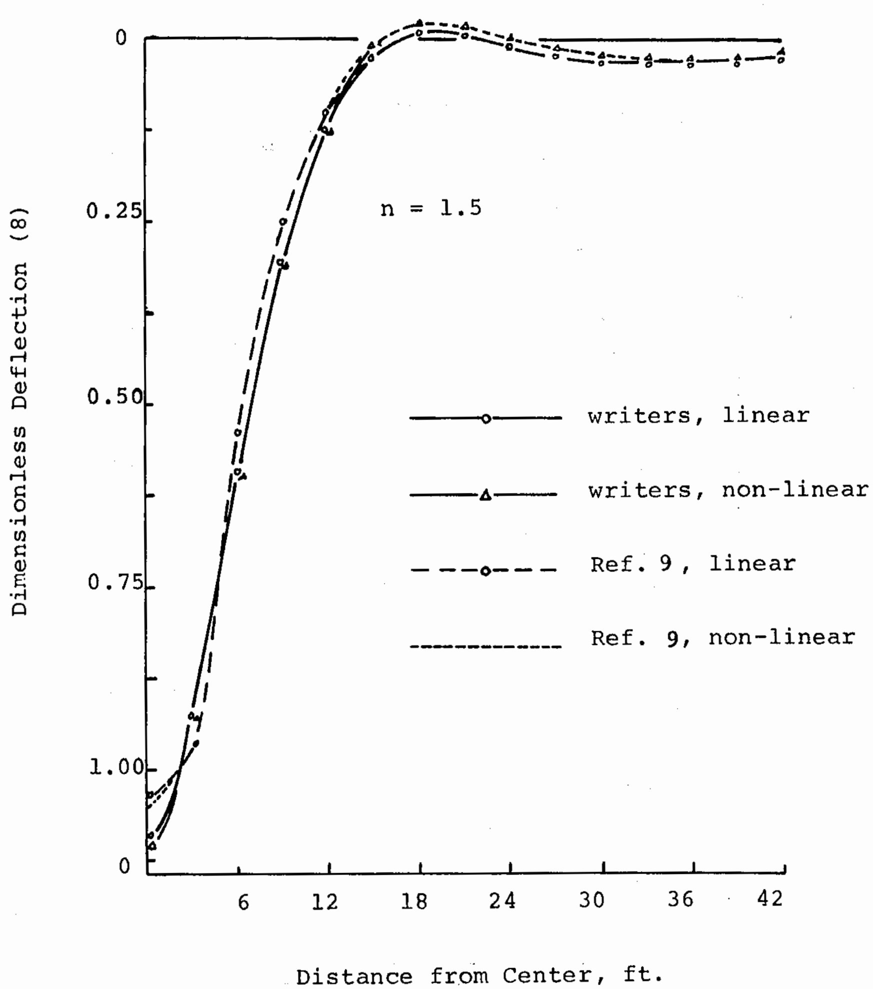

Fig. 10 Comparison of Linear (Tension Allowed) and Non-linear (Tensionless) Solutions for Example 3, $Q = 12.9^k$

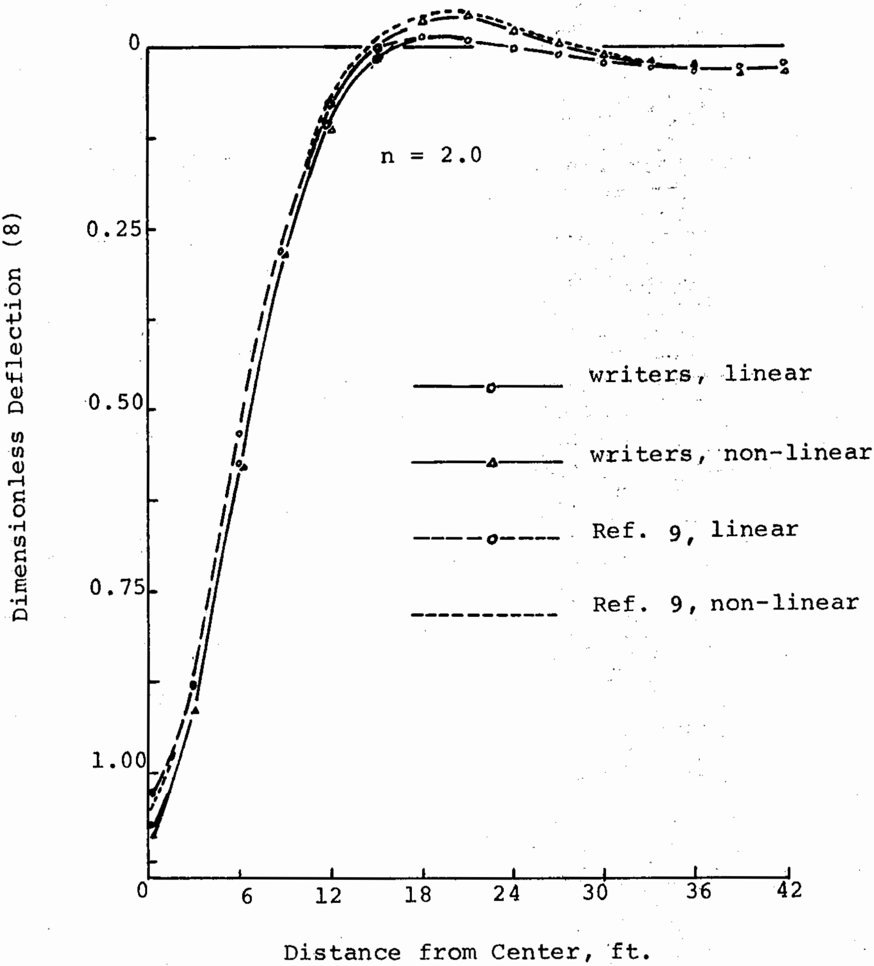

Fig. 11 Comparison of Linear (Tension Allowed) and Non-linear (Tensionless) Solutions for Example 3, $Q = 17.2^k$

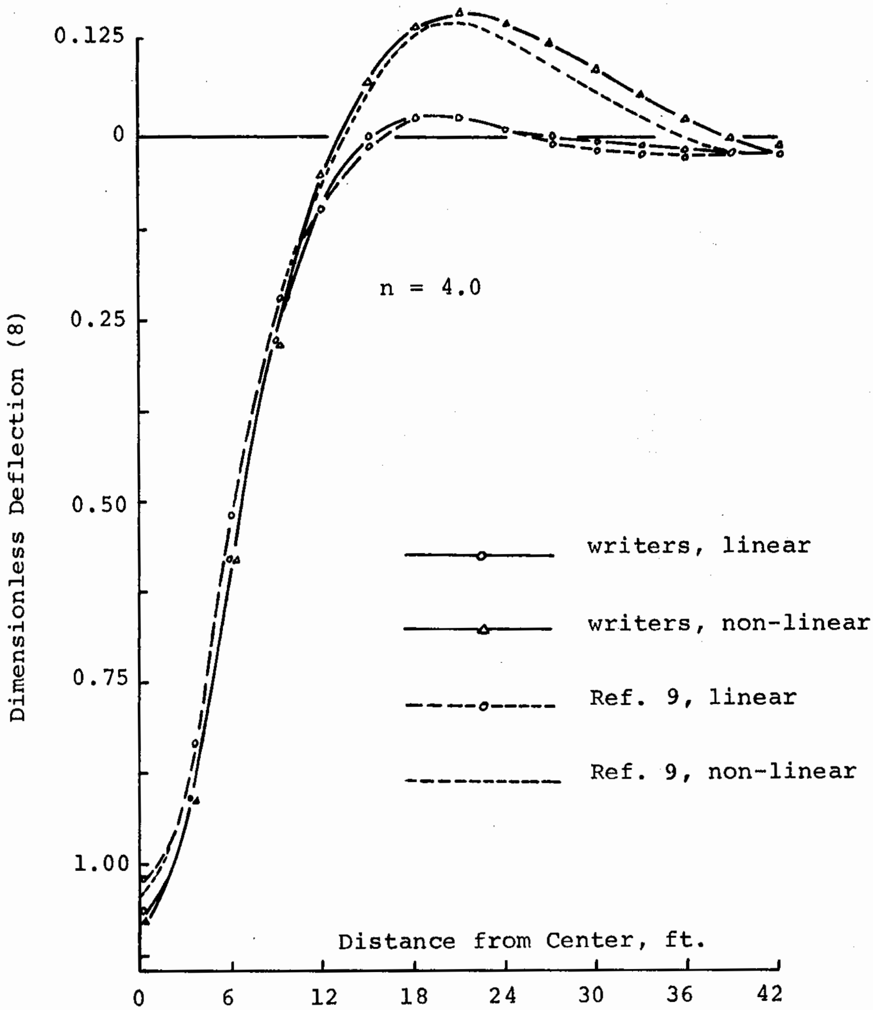

Fig. 12 Comparison of Linear (Tension Allowed) and Non-linear (Tensionless) Solutions for Example 3, $Q = 34.4^k$

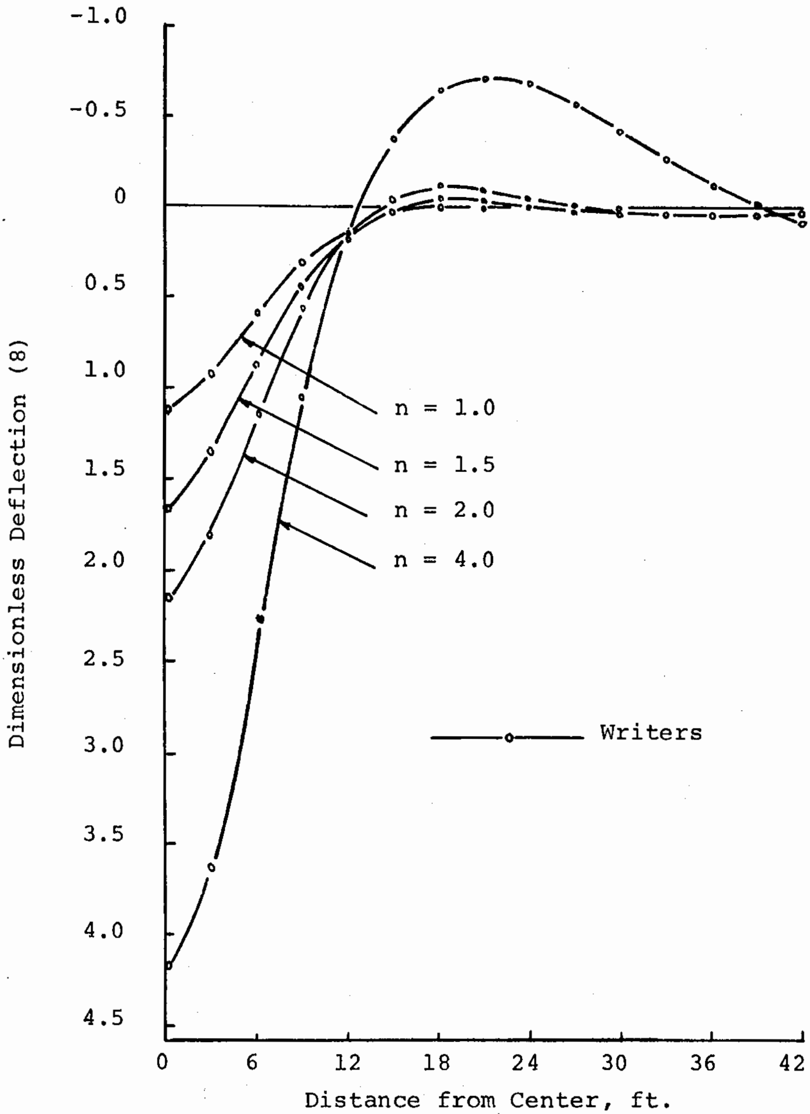

Fig. 13 Dimensionless Deflections, Summary of Load Cases for Example 3.

Summary and Conclusions

A method for determining the reaction pressures of beams subjected to dead weight and concentrated loads and supported on linearly elastic foundations which are unable to support tension has been presented. The supporting medium which is represented by a series of closely spaced springs may be continuous or discontinuous. The method may be readily modified to handle subgrades which exhibit non-linear force-deformation characteristics and/or non-homogeneous soil conditions. The method may also be extended quite easily to solve problems of mat or raft foundations subjected to numerous column loads and moments.

The following conclusions may be drawn:

1. The proposed method of analysis which is an application of a well-known technique in structural analysis is quite straight-forward and may be incorporated easily into a computer program.

2. The discrete solution presented is in good agreement with other solutions (4), (7), (9) for the cell lengths chosen in the examples. Better agreement may be expected if the cell lengths are decreased (more springs used) but the computer running time will increase.

3. Due to the non-linearity of the problem, superposition is not valid. This is illustrated in Example 3 (Fig. 13).

APPENDIX I. – REFERENCES

1. E. Winkler, *Die Lehre von der Elastizitat und Festigkeit,* Prague, Czechoslovakia, 1867.
2. M. Hetenyi, *Beams on Elastic Foundation,* The University of Michigan Press, Ann Arbor, 1946.
3. M. A. Biot, "Bending of an Infinite Beam on an Elastic Foundation", *Journal* of Applied Mechanics. American Society of Mechanical Engineers, March 1937.
4. A. B. Vesić, "Model Studies of Beam Resting on a Silt Subgrade", *Journal* of the Soil Mechanics and Foundations Division, American Society of Civil Engineering, Feb., 1963, Part I.
5. Z. Levinton, "Elastic Foundations Analyzed by the Method of Redundant Reactions", *Trans.* American Society of Civil Engineers, 1949.
6. H. Malter, "Numerical Solutions for Beams on Elastic Foundation", *Trans.* American Society of Civil Engineers, 1960.
7. Joseph E. Bowles, *Foundation Analysis and Design,* MacGraw-Hill Co., New York, 1968.
8. Matlock, Hudson, "Applications of Numerical Methods to Some Problems in Offshore Operations", First Conference on Drilling and Rock Mechanics, University of Texas, 1963.
9. Nien-chien Tsai and Russell A. Westmann, "Beam on Elastic Foundation", *Journal* of Engineering Mechanics Division, American Society of Civil Engineers, October 1967.
10. S. Timoshenko, *Strength of Materials, Part II,* K. Van Nostran Co., Princeton, N.J., 1965.
11. C.K. Wang, *Matrix Methods of Structural Analysis* International Texbtook Co., 1966, Chapter 4 and Chapter 10.

APPENDIX II. – NOTATION

The following symbols are used in this paper:

A	=	transformation matrix
B	=	width of beam
E_s	=	modulus of elasticity of soil
EI	=	flexural rigidity of beam
K	=	spring constant
K_s	=	subgrade modulus
K_s'	=	K_sB subgrade modulus including the effect of the beam width
L	=	total length of beam
ν	=	Poisson's ratio
P	=	joint load matrix
Q	=	magnitude of concentrated center load
S	=	stiffness matrix
X	=	joint deformation matrix
a	=	cell length of beam-foundation
n	=	loading parameter
n_c	=	number of cells in the beam
γ	=	unit weight of beam

COASTAL ENGINEERING AND THE DEVELOPMENT OF BOSTON HARBOR

by

R. H. Cross*, G. J. Vicens**, and T. W. Sy***

Abstract

The limitations imposed on the development of Boston Harbor by coastal phenomena are important considerations in the planning process. Wave erosion can require rip-rap or seawalls around landfills, and restricts the creation and modification of beaches. Storm waves, in conjunction with high astronomical and storm tides, fix the minimum elevation of landfills, causeways and bridges. The navigation and docking of small craft limit allowable tidal currents, thus limiting landfill configurations, and require areas sheltered from wave action. Waves also can interfere with water-based construction activity.

Introduction

Boston Harbor, with its numerous islands, channels and bays, presents many opportunities for development. Such development may include landfills, causeways, bridges, channel realignments, marinas, and other modifications to the natural configuration of the harbor.

Engineers, architects and planners investigating possible developments of this harbor space must consider from the beginning the limitations imposed on projects in the harbor by the natural phenomena associated with the marine environment. This environment influences the development of the Boston Harbor space in several ways:

1. Waves cause erosion of the shoreline, requiring coastal protection. Generally, this protection consists of a cover layer of rock rip-rap along the shoreline, or, at points of severe wave attack, sea walls, as at the northeast end of Long Island.
2. Waves also affect beaches, causing both a seasonal onshore-offshore movement of sand and a longshore drift. (See the section on the construction of beaches.)
3. Marinas and other docking or anchorage facilities need to be designed to provide adequate protection for moored boats and floats.

*Alpine Geophysical Associate, Inc., Norwood, N.J.; formerly Assistant Professor of Civil Engineering, M.I.T.

**Graduate Student, Civil Engineering, M.I.T.

***Graduate Student, Civil Engineering, M.I.T.

4. Extreme storm waves, especially in conjunction with "storm tides", a combination of high astronomical tides and wind-induced tides, can overtop seawalls and embankments, causing flooding of land areas behind.
5. Tidal currents in excess of 3 knots in channels can be a hazard to navigation. Since tidal currents are affected by the shoreline and bottom configuration, this places constraints on landfill arrangements and channel closures.
6. Wave action can interfere with water-based construction activities. Barges, dredges, and floating cranes cannot function safely or effectively in waves higher than about 2-6 ft., depending on the size of the equipment and the wave period.

The above limitations are imposed essentially by three natural phenomena: waves, tides and currents. The nature and effects of each are considered in detail below.

I. Waves

Waves in the harbor arise from three sources: ocean-generated storm waves, ship waves, and waves generated locally by winds in the harbor.

Ocean wave data[1] for Nausett Beach, Cape Cod, have been obtained from the U.S. Army Corps of Engineers. By eliminating waves from the SSE and south, adjustments for the sheltering effect Cape Cod has on Boston can be made. The adjusted data, shown in Figures 1 and 2, describe approximately the ocean waves well outside the harbor, in depths greater than 100 feet or so. The data are presented as the approximate number of hours per year the waves were in each height and period range. The values reported, except ship waves, give the significant wave height, often written $H_{1/3}$. This is defined as the average of the highest 1/3 of the waves in a record, and is related to the maximum, etc., by the following:

$$H_{1/10} = 1.27\, H_{1/3}$$

$$H_{max} = 1.67\, H_{1/3}$$

Wave heights estimated visually usually correspond to the significant height.

[1] These data were obtained from past weather records and used as the basis for wave forecasts. Assuming the weather statistics do not change, the wave statistics produced can be applied to future years.

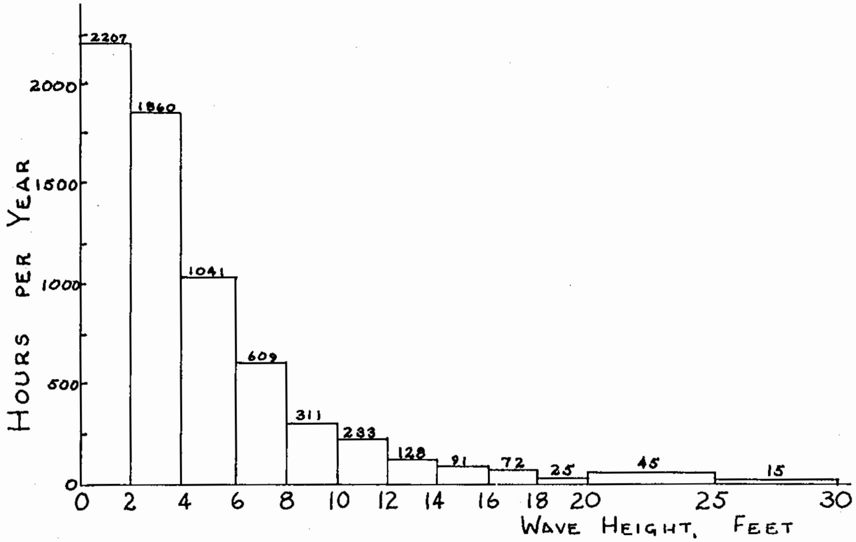

Fig. 1 Wave Heights off Boston Harbor.

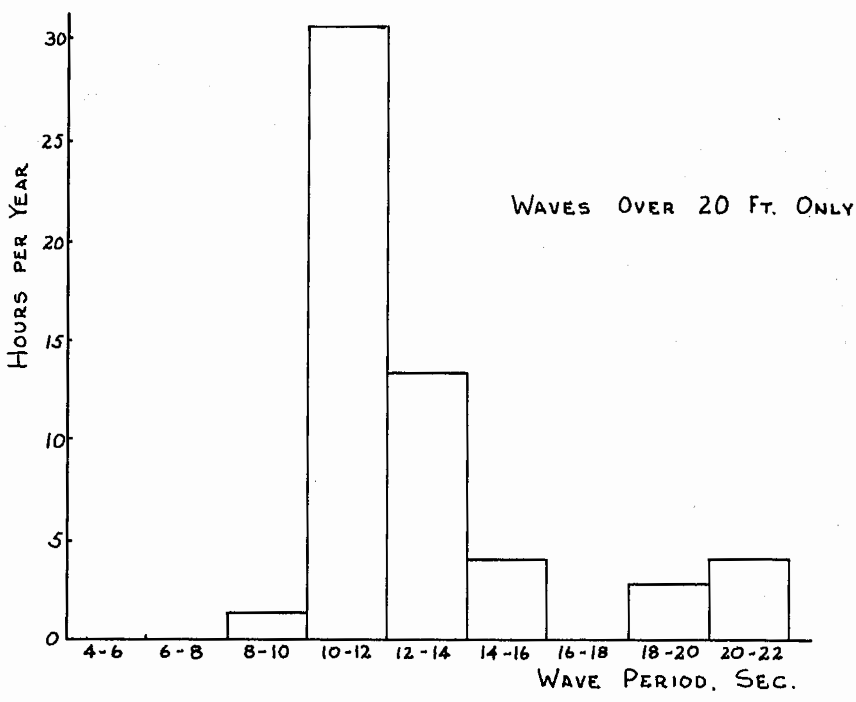

Fig. 2 Wave periods off Boston Harbor.

The speed of a wave in shallow water decreases with decreasing water depth. Thus ocean waves approaching the harbor are refracted by the irregular bottom configuration, with the incident wave energy being focused on islands, shoals and headlands – particularly Outer Brewster (and, to a lesser extent, the other Brewster Islands), Shaf Rocks, and Green Island. A good deal of wave energy is transmitted into the harbor, however, through the major channels – President Roads and Nantasket Roads. In his historical book on the "Islands of Boston Harbor", E. R. Snow mentions "Breakers 40 feet high. . .sweeping right across the mile-wide area between Deer and Long Islands. . ." during a major storm. Once inside the harbor, this wave energy is spread out, and the heights reduced significantly. It is not possible, at present, to predict with any reasonable decree of accuracy the quantitative effect of ocean waves inside the harbor. Further investigation is definitely required. From the navigation chart for Boston Harbor (U.S.C. & G.S. Chart No. 246), however, one can identify several areas inside the harbor likely to be subject to waves at least 60-70% as high as those outside the harbor. For a storm producing waves 30 feet high in the ocean, which Figure 1 indicates may occur once or twice each year, Figure 3 shows the areas that may be subject to waves 20-30 feet high ($H_{1/3}$). More accurate predictions, and predictions of ocean wave heights farther in the harbor and their frequency of occurrence, will require further study.

Locally-generated wave heights can be estimated for various locations, based on the wind speed and fetch (distance over which the wind blows, upwind from the point of interest). These estimates are given in Table I for Spectacle, Thompson and Long Islands, and apply just offshore of the windward side of the island, as indicated by the wind direction shown. The wind speeds were arbitrarily chosen to represent a stiff breeze of frequent occurrence, a storm occurring perhaps yearly, and an occasional hurricane, respectively.

Ships' waves, for vessels of all types traveling at speeds less than 8 knots, are generally less than a foot high, and generally less than two feet for speeds up to 12-14 knots.

Shore Protection

Ship waves are only of significance in interior, well-protected channels, where their height may be exceeded only by rare storms. For protecting new fill areas from erosion, a design wave height of two feet should be used. Banks built on a slope of two horizontal to one vertical or flatter can be protected by a layer of heavy rock perhaps two feet thick, and extending from 2-3 ft. below MLW to the level of the fill, or at least to 15 ft. above MLW.

Since a storm passing Boston generates both ocean waves and waves inside the harbor, waves from both sources need to be considered simultaneously. While the ocean waves have periods in the range 10-14 sec. (Figure 2), locally-generated storm waves have periods in the 3-5 sec. range. It is not

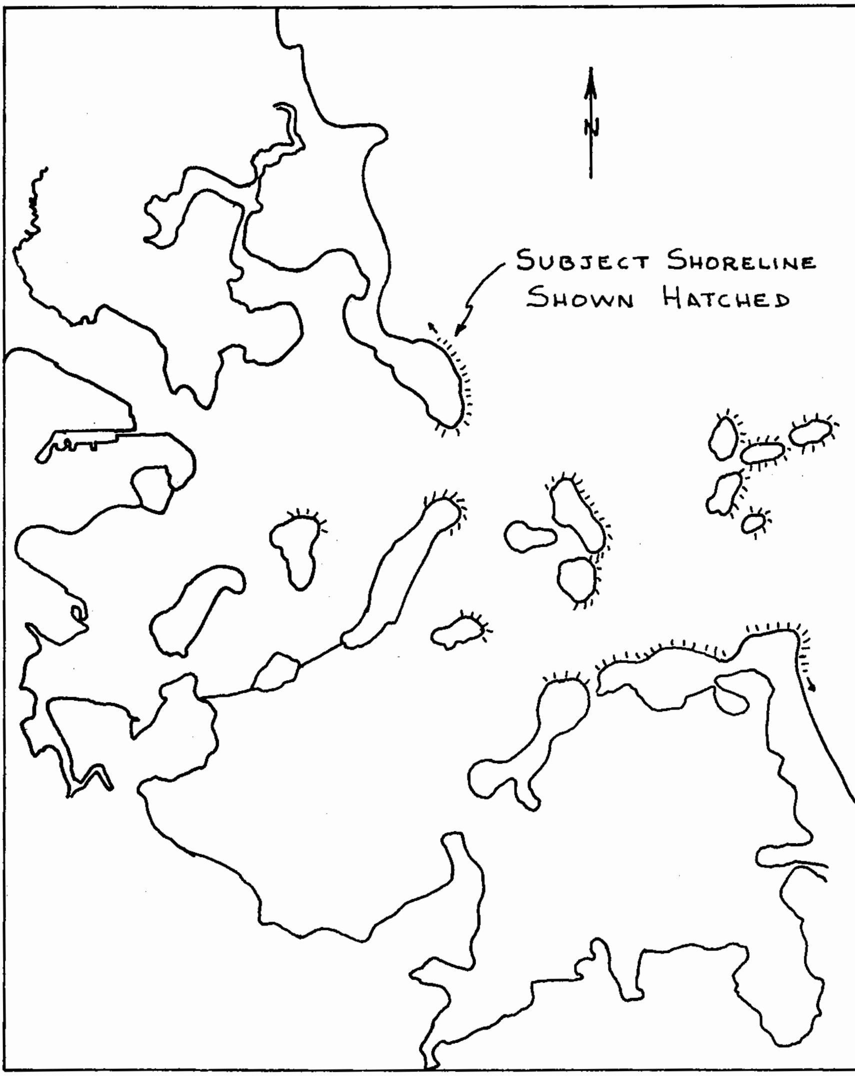

Fig. 3 Areas Subject to Severe Wave Action - Boston Harbor

Table I – Locally Gen. Waves

Location	Wind Dir.	Fetch Naut. Mi.	Wind Spd. Knots	$H_{1/3}$ Ft.	$T_{1/3}$ Sec.
Spectacle Is.	N	1.3	20	< 2	2.3
			50	3.7	3.5
			90	6.8	4.6
	NE	1.4	20	< 2	2.3
			50	3.7	3.5
			90	6.8	4.6
	E	0.8	20	< 2	2.2
			50	3.2	3.2
			90	6.2	4.0
Thompson Is.	NE	1.8	20	< 2	2.5
			50	4.2	3.7
			90	9.0	5.1
	NW	0.8	20	< 2	2.2
			50	3.2	3.2
			90	6.2	4.0
Long Is.	NW	1.8	20	< 2	2.5
			50	4.2	3.7
			90	9.0	5.1
	SE	1.6	20	< 2	2.5
			50	4.0	3.7
			90	8.0	4.8

understood how these interact. In the area around Thompson Island, the locally-generated waves run up to 4 ft. in the largest "annual" storm; probably the ocean waves are approximately the same height. For a 6-ft. design wave, at a tide level of +12 ft., erosion protection for new fill areas can be provided for a slope of 2:1 or flatter by a 2 to 3 foot layer of rock extending from 6 ft. below MLW to 18 ft. above, at a cost of perhaps $35-50 per foot of shoreline for a 2:1 slope, $70-100 for a 4:1 slope, if the rock can be trucked to the site and dumped; the cost doubles if the rock has to be barged to the site. More exposed locations may require a raised embankment to prevent flooding, while more sheltered locations would require less rock. The figures given above are, therefore, only general costs for protecting fill areas.

Marinas and Other Docking Facilities

Small-craft shelter requirements vary, depending on the type of mooring (rigid, as wharfs and finger piers, or an anchorage) and the use. Pleasure craft at a rigid mooring will likely sustain damage from waves over 1-2 ft. high, depending on the size of the craft, the wave steepness (long swells or chop – chop is worse), and the skill of the boat owner in tying the boat. Boats at a properly designed mooring with room to swing can ride out nearly any sea that they could handle underway. The large amount of space required for moorings, however, limits the use of anchorages in many parts of Boston Harbor. Marinas in virtually all parts of the harbor need to be partly enclosed by fill or by a breakwater to provide proper protection.

A breakwater built to 18 ft. above MLW, in water 10 ft. deep at MLW, with 1.5:1 side slopes, will cost approximately $1000-1500 per linear foot. In general, permanent docking along pile-supported causeways is not recommended. However, the western and southwestern sides of filled causeways will, in most cases, be adequately protected. Fair-weather docking at most sites will require no protection, except that such facilities on the outer islands should be on the west or southwest sides of the islands, in coves where possible.

Beaches

A beach is not just an inert heap of sand that happens to be at the water's edge. The action of the waves on the sand keeps the beach in a continual state of flux. Basically, there are two main modes of transport: onshore and offshore, and longshore drift. The onshore-offshore movement on natural beaches generally occurs in an annual cycle. Steep waves from the winter storms tend to move material from the beach to deeper water where it forms offshore bars, while the gentler summer swells tend to move it back on shore. The exact mechanisms involved are not well understood, but the fact that this happens is well documented[1] Many a wide summer beach disappears almost entirely in the winter to reappear the next summer.

More serious is the longshore movement of sand, called "littoral drift". This is caused by waves breaking at an angle to the beach, and moving the sand in the direction of the longshore component of the wave advance. The quantities transported can be considerable – at one California beach, the rate is estimated at 300,000 cu.yd./year southward. This is nearly a ton of sand per minute.

Man-made structures disrupt the longshore flow of sand. A single jetty, or groin, built out from the beach will trap sand on the upcoast side, while erosion is increased on the downcoast side. If many of these groins are spaced along the shore, they allow the beach to re-align itself more perpendicular to the direction of approach of the prevailing waves, thereby lessening the transport rate. A groin, however, never created a single grain of sand; you have to have a supply to begin with, and there are virtually no sources in Boston Harbor. However, littoral transport of the past has left its mark on many of the harbor islands: rocks and cliffs on the exposed sides, tapering off to gravel, sand, or mud on the sheltered sides.

The rate of movement of sand, both onshore-offshore and longshore – depends on the intensity of wave action. In protected locations, it may be possible to construct beaches and maintain them at relatively low cost. The presence of mud and other fine sediments in many of the more protected portions of the harbor, however, suggests that a nice sand beach may become contaminated with mud fairly rapidly. In more exposed locations, the waves which move the sand about also tend to keep it clean.

For example, on Long Island the present configuration of the shoreline and adjacent areas suggest that sand would move to the southwest, since most waves come from the east and northeast; on the southeastern side of the island, it would probably end up in the deep channel, while on the northeastern side, Moon Head would possibly trap some. It might be possible to reduce the transport rates sufficiently by constructing groins along the shore, but more detailed studies would be required to determine the costs involved, both for initial construction and for maintenance. The Corps of Engineers accepts responsibility for maintaining natural public beaches; whether they would do so for constructed beaches is open to question.

For a very rough initial cost estimate for beach construction, using sand with a median diameter of 1 mm and a beach slope of 1:5, with a beach 60 yd. wide (with approximately half the beach below the high tide mark), and 1 yd. thick, at $2.50/yd. for sand, gives approximately $200. per linear yard of beach.

[1] A readable and competently written book on the subject is "Waves and Beaches" by Willard Bascom, available in paperback.

II. Tides and Storm Tides

The principal datum planes and selected tide levels are related to the Boston Low Water Datum as shown in Table II. These data indicate a 1-ft. rise in sea level by the year 2020; this should be taken into account in the design of fill elevations.

The waves and storm tides basically determine the elevation to which fill must be made. Considering the highest tide of record, 15 ft. above MLW, and allowing for a 1-ft. rise in sea level and 2 feet for drainage assurance, gives a ground elevation of +18 ft. above MLW, or approximately 13 ft. above the MSL datum of the U.S.G.S. topographic maps.

Table II – Datum Planes and Tide Levels

Highest tide of record (1951)	15.0 ft.
Mean high water (1941-59)	9.8 ft.
Mean tide level (1941-59)	5.05 ft.
Projected mean tide level, year 2020	6.0 ft.
Mean sea level (U.S.G.S. Datum)	4.87 ft.
Boston low water datum	0.00 ft.
Boston City Base	-0.78 ft.
Lowest tide of record	-3.48 ft.

Along exposed portions of the shore, a higher embankment should be provided to protect against wave overtopping and flooding. More detailed information on wave statistics, proposed shoreline configurations, and suggested land uses (i.e., susceptibility to damage) is needed before estimates can be given; however, if a cost of $50. per linear foot of shoreline is used for protection for all fill areas, the variations should average out.

Structural causeways should be built to clear the highest waves expected, at the highest tide level, both to prevent damage and to assure use of the causeway during storms. For most locations, a clear elevation of 22-24 ft. above MLW to the underside of the span should suffice; for areas such as between Castle and Spectacle Islands, or Spectacle and Long Islands, however, this should be increased to 28-30 ft. Filled causeways similarly should not flood excessively during severe storms, unless alternate emergency access is available. With alternate routes, roadway elevations of 16-18 ft. above MLW are acceptable; without, 20-24 ft. should be used. Both figures should be increased by 5 ft in exposed locations such as those mentioned above. Filled causeways require the same protection from erosion as other fill areas.

III. Harbor Currents

Harbor currents under present conditions are given in the U.S.C. & G.S. publication "Tidal Current Charts – Boston Harbor". An examination of these charts, in conjunction with the navigation charts, gives a good indication of the principal flows in the harbor.

The three constraints posed by tidal currents are as follows:

a. Closing off channels carrying significant volumes of water will tend to increase velocities in other channels providing water to the same basins. These increased velocities can be calculated from the current charts and navigation charts by assuming that the same volume of water still enters and leaves the basin with the tides. Currents in excess of 3 knots (5 ft./sec.) are considered hazardous to small craft.

b. In constructing enclosed basins for marinas, the surface area of the basin and the tide range indicate the required entrance cross-section, both to prevent erosion of the inlet and to keep tidal velocities less than 3 knots.

Approximate values are given in the table below.

Basin Surface Area, Acres	Entrance Cross-Section Below Mid-Tide Level, ft.^{2}
3	60
10	200
30	500
100	1,400
300	4,000
1,000	10,000

The flow velocities here range from 1.5 to 3 ft./sec. in the inlet.

c. Tidal flows must be adequate to prevent the concentration of pollutants, and to nourish shellfish.

Since it is anticipated that most transportation links between islands would be pile-supported causeways, which do not impede tidal currents, no significant changes in tidal flows are foreseen. Three possible fill causeway links – Squantum-Thompson Island, Thompson-Spectacle Island, and Moon Head-Long Island – would not close off channels transporting significant volumes of water. Thus closing any two of these gaps would not be likely to have any serious consequences. One of the three should be left open to assure flushing of the enclosed shallow zone.

Conclusion

The above data and estimates are intended to indicate some of the engineering restrictions on harbor development that should be considered in the early planning stages. They are, of necessity, very general. As the planning process proceeds to the consideration of specific, detailed projects, competent engineering would be required to define the specific requirements and associated costs for each proposal.

PROCEEDINGS OF THE SOCIETY

Minutes of Meeting

Boston Society of Civil Engineers

May 19, 1971.– The Boston Society of Civil Engineers held its regular monthly meeting at the New England Life Building, 225 Clarendon Street, Boston, Mass. A social hour at 5:30 and a roast beef dinner served at 6:30 P.M., at which thirty-nine (39) persons were seated preceded the business meeting.

President Ernest A. Herzog convened the regular business meeting at 7:40 P.M. He stated that the minutes of the March 24, 1971 meeting would be published in a forthcoming issue of the Journal and that the reading of those minutes would be waived unless there were objections.

President Herzog announced with regret, the death of the following members:

Matthew H. Chamberlain, elected a member April 5, 1952, who died Nov. 17, 1970

Frederick D. Goode, elected a member Dec. 20, 1950, who died Nov. 24, 1970.

Henry A. Mohr, elected a member April 13, 1933, who died Feb. 22, 1971.

George A. McKenna, elected a member Feb. 14, 1954, who died Aug. 25, 1970.

Frank K. Perkins, elected a member June 21, 1944, who died Feb. 6, 1971.

George C. Woods, elected a member Dec. 15, 1958, who died Sept. 16, 1970.

Albert A. Adelman, elected a member Feb. 16, 1944, who died May 14, 1971.

The members stood for a moment of silence in tribute to the deceased.

The Secretary announced that applications for membership had been received from the following:

Walter L. Abel, Medford, Mass.
William J. Comeau, Lynn, Mass.
D. Joseph Hamel, Natick, Mass.
Richard W. Long, Bridgewater, Mass.
Robert J. McDonagh, Hingham, Mass.

President Herzog stated that this was a joint meeting with the BSCE and ASCE Transportation Sections. He called upon A. Russell Barnes, presently chairman of both sections, to conduct any business of those sections. Mr. Barnes declared that there was no formal business to be conducted.

President Herzog then turned the podium over to Mr. Barnes to introduce the speaker of the evening. The speaker was Mr. Guy D. Rosmarin, Transportation Advisor to the Governor, Commonwealth of Massachusetts, whose subject was "The Politics of Transportation – 1971". Mr. Rosmarin related the expansion of the transportation system from the time of the Mexican War – about the time that the Boston Society of Civil Engineers was founded. He carried forward the development of transportation to the present time. In his talk he highlighted the difficulties that the cities are facing, and the related transportation problems. He pointed out that large expenditures have been made for highways in the urban renewal areas, but that little had been done to improve transportation facilities for the residents of those areas. Mr. Rosmarin made an effort to present the problems as he saw them, and suggested some possible solutions. Following his talk, there was a lengthy, spirited, and stimulating question and answer period.

Forty-six members and guests were present at the business meeting.

The meeting adjourned at 9:00 P.M.

Respectfully submitted,

Paul A. Dunkerley
Secretary

June 2, 1971.– The regular monthly meeting of the Boston Society of Civil Engineers was held at the Tech House Restaurant, 545 Main Street, Cambridge, Mass., following the annual Sanitary Section outing, which this year consisted of a trip to the MDC Water Detention and Chlorination Station on Memorial Drive in Cambridge; and also a trip to the M.I.T. Nuclear Reactor in Cambridge. A social hour at 5:30 P.M., was followed by a buffet dinner at 6:30 P.M.

At 7:30 P.M., in the absence of President Herzog, Secretary Paul A. Dunkerley called the meeting to order. Secretary Dunkerley stated that the minutes of the May 19, 1971 meeting would be published in a forthcoming issue of the Journal, and that the reading of those minutes would be waived unless there were objection. There were no objections.

Secretary Dunkerley also announced that applications for membership had been received from the following:

Chan K. Lin, Brookline, Mass.
Jackson T. K. Ho, Chestnut Hill, Mass.
Ahmad B. Newab, Belmont, Mass.
John R. Chesebro, Franklin, Mass.

Secretary Dunkerley then called upon Mr. Cornelius J. O'Leary, Chairman of the Sanitary Section, to conduct any necessary business. Mr. O'Leary conducted a brief business meeting of the Section, and then introduced the speaker for the evening.

The guest speaker for the evening was Mr. K. Peter Devenis, Charles A. Maguire & Associates, Inc. He gave a very interesting slide-illustrated talk on "Storm Detention and Chlorination Station near B.U. Bridge", which had been the subject of the afternoon outing. Mr. Devenis explained the physical features of the station, and what the station hoped to accomplish in the process of cleaning up the waters of the Charles River. Mr. Devenis also related this particular Detention and Chlorination Station to the overall Master Plan for the Disposal of Liquid Wastes in the Metropolitan Boston Area. A brief question and answer period followed Mr. Devenis' talk.

Thirty-six members and guests were present at the buffet dinner and the meeting following.

The meeting adjourned at 8:15 P.M.

Respectfully submitted,

Paul A. Dunkerley
Secretary

BOSTON SOCIETY OF CIVIL ENGINEERS

COMMITTEES 1971-1972

NOMINATING COMMITTEE

John M. Biggs

Leslie J. Hooper
Charles A. Parthum
Frank E. Perkins
Albert B. Rich
(Term Expires 1972)

Harry L. Kinsel
Stephen E. Dore, Jr.
David A. Duncan
Howard Simpson
(Term Expires 1973)

PROGRAM COMMITTEE

Ernest A. Herzog, Chairman
Cornelius J. O'Leary
Sepp Firnkas
A. Russell Barnes
Albert G. Ferron

James P. Archibald
Max D. Sorota
Paul A. Dunkerley
H. Hobart Holly

Philip A. Wild
Morse Klubock
Alan Rimer

PUBLICATION COMMITTEE

Max D. Sorota, Chairman
William A. Henderson
Philip A. Wild
Albert G. Ferron
James P. Archibald

H. Hobart Holly
Cornelius J. O'Leary
Sepp Firnkas
A. Russell Barnes

Simon Kirshen
Morse Klubock
Alan Rimer

LIBRARY COMMITTEE

George W. Hankinson, Chairman

Robert H. Culver

Robert L. Fuller

HOSPITALITY COMMITTEE

Peter K. Taylor, Chairman

Conrad Fagone
Charles E. Fuller

Philip A. Bianchi
Samuel E. Rice, 3rd.

MEMBERSHIP COMMITTEE

Edmund G. Johnson, Chairman
A. Paul LaRosa

Gerald L. Woodland
William S. Zoino

Charles H. Flavin
Richard F. Battles

ADVERTISING COMMITTEE

Samuel E. Rice, 3rd, Chairman

Ronald E. Bucknam
H. Hobart Holly

Walter M. Newman
Max D. Sorota

QUARTERS COMMITTEE

James P. Archibald, Chairman
Robert T. Colburn

Robert H. Culver
Paul A. Dunkerley

Max D. Sorota
David A. Duncan

BY-LAWS COMMITTEE

Paul A. Dunkerley, Chairman
Edward C. Keane

Robert T. Colburn

Frank L. Heaney

A.S.C.E.—B.S.C.E. RELATIONS

James P. Archibald, Chairman
Edward C. Keane

William A. Henderson

Robert J. Van Epps

JOHN R. FREEMAN FUND

Leslie J. Hooper, Chairman
Clyde W. Hubbard
George R. Rich

David R. Campbell

Lee M.G. Wolman

RALPH W. HORNE FUND

William L. Hyland, Chairman

George G. Bogren

Miles N. Clair

THOMAS R. CAMP FUND

Robert H. Culver, Chairman

Cornelius J. O'Leary

Albert G. Ferron

FITZGERALD-HERSCHEL AWARD

Peter S. Eagleson, Chairman

Edward C. Keane

Saul Namyet

SANITARY SECTION AWARD

Robert L. Meserve, Chairman

William C. Traquair

Charles Y. Hitchcock, Jr.

STRUCTURAL SECTION AWARD

Richard C. Jasper, Chairman

Robert L. Fuller

Frank J. Heger

TRANSPORTATION SECTION AWARD

H. Lowell Crocker, Chairman

Charles D. Shaker

Edward C. Keane

HYDRAULICS SECTION AWARD

Lawrence C. Neale, Chairman

Lee M.G. Wolman

Allan T. Gifford

CONSTRUCTION SECTION AWARD

Paul S. Crandall, Chairman

William E. Wiley

Frank J. Killilea, Jr.

GEOTECHNICAL SECTION AWARD

Horst Borbereky, Chairman

Harl P. Aldrich, Jr.

Donald T. Goldberg

COMPUTER SECTION AWARD

Frank E. Perkins, Chairman

Gerald L. Woodland, Jr.

Charles L. Miller

JOINT LEGISLATIVE COMMITTEE

Charles A. Parthum, Chairman

Joseph C. Knox

Cornelius J. O'Leary

SUBSOILS OF BOSTON COMMITTEE

Horst Borbereky, Chairman

Richard F. Battles
Donald T. Goldberg

James F. Haley
Rev. Daniel Linehan

PUBLIC RELATIONS COMMITTEE

Ernest A. Herzog, Chairman

Peter S. Eagleson

Walter M. Newman

AUDITING COMMITTEE

Peter S. Eagleson

Lawrence C. Neale

INVESTMENT COMMITTEE

Robert T. Colburn, Chairman

Ernest A. Herzog

James P. Archibald